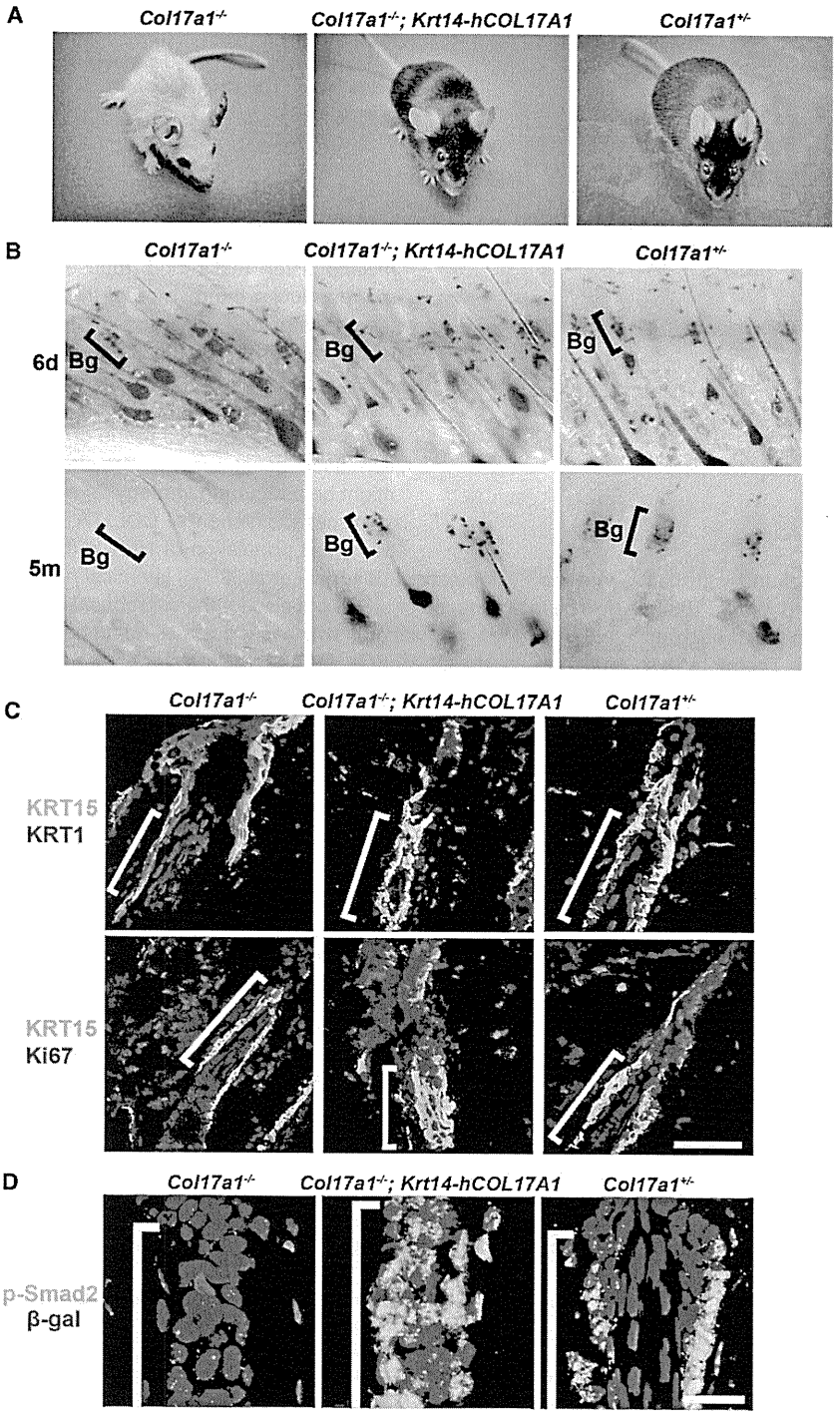

Figure 6. Transgene-Mediated Correction of *COL17A1* Expression in *Col17a1*$^{-/-}$ Basal Keratinocytes Rescues the Loss of MSCs

The *Krt14-hCOL17A1* transgene was introduced into *Col17a1*$^{-/-}$ mice.

(A) Macroscopic phenotype of 7- to 9-month-old *Col17a1*$^{-/-}$ mice with the *Krt14-hCOL17A1* transgene and *Col17a1*$^{+/-}$ mice.

(B) Distribution and morphology of *Dct-lacZ*-expressing melanoblasts in the bulge area (Bg) are normalized by the *Krt14-hCOL17A1* transgene in *Col17a1*$^{-/-}$ mice. Bulge-subbulge areas are demarcated by brackets.

(C) Ectopic KRT1 expression and abnormal proliferation of HFSCs in the bulge-subbulge area (brackets) are corrected by the *Krt14-hCOL17A1* transgene in *Col17a1*$^{-/-}$ mice. These mice were observed at 13 weeks of age during the anagen phase. Scale bar represents 50 μm.

(D) The downregulated expression of phospho-Smad2 (in green) in *Col17a1*$^{-/-}$ HFSCs and MSCs within the bulge-subbulge areas (demarcated by brackets) was also normalized by forced expression of the *Krt14-hCOL17A1* transgene in *Col17a1*$^{-/-}$ keratinocytes. Dct-lacZ-expressing melanocytes in the bulge area are shown in red. Scale bars represents 20 μm.

See also Figure S6.

with mechanical stress. Although mechanical stress, such as attempts to peel the neonatal mouse skin, can induce skin erosion or blistering in *Col17a1*-null mice (Nishie et al., 2007), it did not significantly accelerate hair graying or hair loss in these mice. Importantly, we did not find evidence of macroscopic/microscopic junctional separation, basal cell death, nor inflammatory cell infiltrates between the HFSCs and the basement membrane in *Col17a1*-null mouse skin. Instead, we found that significant defects in HFSC quiescence and immaturity in *Col17a1*-null mice were the earliest events that could explain the defective maintenance of HFSCs over ensuing hair cycles. These findings underline a critical cell-autonomous role for COL17A1 in the maintenance of HFSCs under physiological conditions. Although we did not detect adhesion defects of *Col17a1*-null keratinocytes on feeder cells used for colony assay in this study, weakening of cell attachment has been found with human cultured keratinocytes treated with COL17A1 antibody under vibration conditions (Iwata et al., 2009). One adhesion-based explanation for the premature HFSC depletion in *Col17a1*-deficient mice is that COL17A1-dependent anchoring of HFSCs to the basal lamina might regulate the quiescence and differentiation of HFSCs by modifying their division frequency and properties. Regardless of the precise mechanism involved, our findings reveal a potential mechanism for the hair loss (alopecia) seen with human *COL17A1* deficiency, which causes the nonlethal form of junctional epidermolysis bullosa, also known as generalized atrophic benign epidermolysis bullosa (GABEB) (McGrath et al., 1995; Nishie et al., 2007). It has been reported that the hair loss in GABEB patients is not always associated with

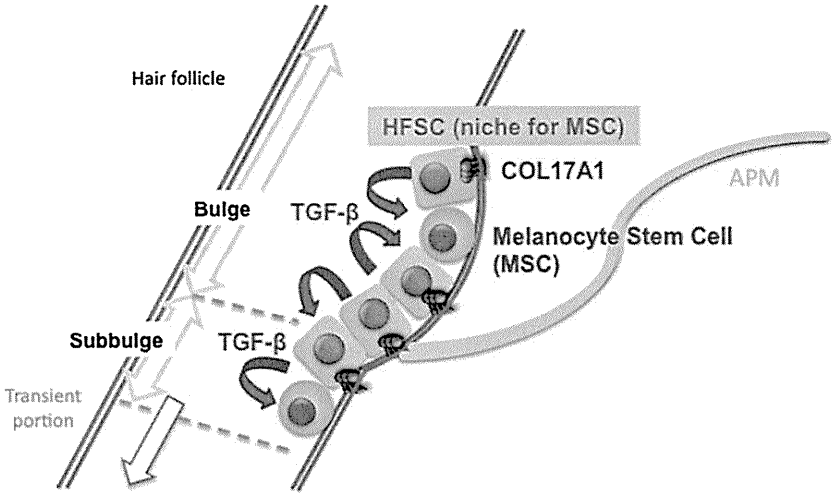

Figure 7. A Schematic Model for HFSCs and MSC Niche
HFSCs provide COL17A1-dependent niche for MSCs though TGF-β signaling. APM, arrector pili muscle.

surrounding skin surface changes but is associated with hair follicle atrophy or hair follicle loss (Hintner and Wolff, 1982). This finding is consistent with the late skin changes such as hair follicle atrophy seen in *Col17a1*-null mice. Therefore, we suggest that this mouse model may be a powerful tool for helping to understand the pathomechanisms of premature alopecia.

Human patients with GABEB also show epidermal atrophy with aging. *Col17a1*-deficient mice show transient epidermal hyperplasia in some focal areas at around 6 months of age (Figure 3D) but the entire skin becomes gradually more atrophic over time. Similar but more pronounced changes have been observed in the setting of stem cell depletion such as is seen in *Rac1* conditional knockout mice (Benitah et al., 2005) and in c-Myc transgenic mice (Arnold and Watt, 2001; Waikel et al., 2001). The late onset of epidermal atrophy seen in *Col17a1*-null mice might represent the eventual depletion or a decreased self-renewing potential of epidermal stem cells for the IFE.

More generally, *Col17a1*-null mice have provided evidence of an unexpected biological function for HFSCs. Although we have previously shown that the niche microenvironment plays a dominant role in fate determination for MSCs (Nishimura et al., 2002), the type of cell and/or the extracellular matrix in the bulge area that comprises the functionally essential component(s) of the niche has been unclear. Our current data indicate that HFSCs serve as a functional niche for MSCs and act through HFSC-derived TGF-β signaling, which is critical for MSC maintenance (Figure 7). It is notable that MSC immaturity was lost in *Col17a1*-deficient mice at a time when HFSCs were undergoing aberrant proliferation and differentiation in the bulge area with gradual loss of HFSC characteristics, including TGF-β production. There are a number of keratinocyte-specific gene-deficient mice that display a hair loss phenotype caused by HFSC depletion (Benitah et al., 2005; Zanet et al., 2005). However, as far as we know, characteristic premature hair graying has not been reported in those mice. It is also interesting that HFSCs nurture MSCs even though they are derived from a completely different developmental origin (Nishimura et al., 1999, 2002). A similar niche function provided by one type of stem cell for another was reported in *Drosophila melanogaster* testis and mouse bone marrow during the revision of this paper (Leatherman and Dinardo, 2010; Méndez-Ferrer et al., 2010; Omatsu et al., 2010). The maintenance of somatic stem cell populations in a coherent cell mass with a specialized tissue organization such as in the hair follicle bulge might be a recurring strategy for somatic stem cell maintenance. COL17A1 in the basal cell population of HFSCs (the α6-integrin^{high} population) (Blanpain et al., 2004) is critical not only for the maintenance of MSCs but also for the suprabasal HFSCs (α6-integrin^{low} population), which suggests a common niche function for basal HFSCs for the maintenance of adjacent MSCs and HFSCs. Further studies to elucidate the precise niche properties of HFSCs may clarify additional fundamental mechanisms for the maintenance of stem cell pools as clustered stem cell populations.

EXPERIMENTAL PROCEDURES

Animals

Dct-lacZ transgenic mice (Mackenzie et al., 1997) (a gift from I. Jackson), *Col17a1*-knockout mice (Nishie et al., 2007), and *Krt14*-human *COL17A1* transgenic mice (Olasz et al., 2007) have been described previously. *Col17a1*$^{+/+}$ and *Col17a1*$^{+/-}$ mice are referred to as control mice. *CAG-CAT-EGFP* mice (a gift from J. Miyazaki) were bred with *Dct*$^{tml(Cre)Bee}$ mice (a gift from F. Beermann) to generate compound heterozygotes as described previously (Osawa et al., 2005). All mice were backcrossed to C57BL/6J. Animal experiments conformed to the Guide for the Care and Use of Laboratory Animals and were approved by the Institutional Committee of Laboratory Animal Experimentation.

TGF-βRII straight knockout mice (a gift from M. Taketo) (Oshima et al., 1996) were bred with Rag2-deficient mice at the Animal Research Facility of the Institute of Medical Science, University of Tokyo. Animal care of the line was carried out in accordance with the guidance of Tokyo University for animal and recombinant DNA experiments.

Histology, Immunohistochemistry, and Flow Cytometry Analyses

Paraffin, frozen sections, and whole-mount β-galactosidase staining were performed as previously described (Nishimura et al., 2002, 2005). Additional details on the methods and antibodies used are provided in the Supplemental Information. Multicolor flow cytometry analysis for HFSCs was performed with a FACSCalibur (BD).

Electron Microscopy

For electron microscopy, 20 μm cryostat sections were cut and stained in X-gal solution for 12 hr at 37°C. The sections were postfixed in 0.5% osmium tetroxide for 30 min, stained with 1% uranyl acetate for 20 min, dehydrated in a graded ethanol series, and then embedded in epoxy resin. Semithin sections (1 μm thick) were examined after toluidine blue staining and were observed by light microscopy. Ultrathin sections were observed with a JEM-1210 transmission electron microscope (JEOL) at 80 KV.

Isolation of Melanocytes

Dorsal skin was harvested from 6-day-old *CAG-CAT-EGFP/+; Dct$^{tml(Cre)Bee/\ tml(Cre)Bee}$* mice. The skin specimens were incubated in PBS containing 300 U/ml dispase (Sanko Junyaku) overnight at 4°C, and then the dermis was removed from the epidermis with a stereomicroscope. The epidermis was further dissociated by treatment with 0.25% trypsin for 10 min at 37°C. After neutralization with fetal calf serum (FCS), GFP$^+$ melanocytes were sorted with JSAN (Bay Bioscience).

RNA Isolation and Reverse Transcriptase Polymerase Chain Reaction

Total RNAs from mouse skin or sorted GFP$^+$ melanocytes were isolated with TRIzol (GIBCO) according to the manufacturer's instructions. 3 μg total RNA was used for cDNA synthesis in THERMOSCRIPT RT-PCR System (GIBCO) according to the manufacturer's instructions. The following primers were used for the analysis: mouse *Col17a1* (forward primer 5′-actcgcctcttcttcaacca, reverse primer 5′-gagcaggacgccatgttatt) and *GAPDH* (forward primer 5′-accacagtccatgccatcac, reverse primer 5′-tccaccaccctgttgctgta).

Colony-Formation and Adhesion Assays

For the colony-forming assay, keratinocytes from newborn mice were used. Dorsal skins were incubated in PBS containing 300 U/ml dispase (Sanko Junyaku) for 1 hr at 37°C, after which the dermis was removed from the epidermis with a stereomicroscope. The epidermis was further dissociated by treatment with TrypLE Select (GIBCO) for 10 min at 37°C. The isolated cells (10^5 per 6 cm dish) were seeded on 3T3-J2 feeder cells treated with mitomycin C. The cells were grown in calcium-free medium (3:1 = calcium-free DMEM:CnT-57CF.S [Celltec]) supplemented with 1.8×10^{-4} M adenine, 1% antibiotic-antimyotic solution (Sigma), 2 mM L-glutamine, 0.5 μg/ml hydrocortisone, 5 μg/ml insulin, 10^{-10} M cholera enterotoxin, 10 ng/ml EGF, and 10% FCS treated with Chelex-100 resin (BioRad) at 32°C in a humidified atmosphere with 8% CO_2 for a total of 14 days. To visualize the keratinocyte colonies, the cells were washed with PBS and were then fixed in 4% formalin for 20 min at room temperature. After further washing in PBS, the cultures were stained for 5 min at room temperature with crystal violet.

For the adhesion assay, isolated keratinocytes (10^5 per well in 6-well plates) were seeded on 3T3-J2 feeder cells treated with mitomycin C or on collagen I-coated 6-well plates. 12 or 24 hr later, keratinocytes was washed three times in PBS and were collected with 0.05% trypsin-EDTA. Collected cells were fixed with 2% formaldehyde for 10 min at 37°C, permeabilized by ice-cold 100% methanol for 30 min, and stained with an Alexa Fluor 488-conjugated pan-cytokeratin monoclonal antibody (EXBIO). Detection of adherent keratinocytes was performed with a FACSCanto II (BD).

SUPPLEMENTAL INFORMATION

Supplemental Information includes Supplemental Experimental Procedures and six figures and can be found with this article online at doi:10.1016/j.stem.2010.11.029.

ACKNOWLEDGMENTS

We thank Dr. Makoto Taketo for *Tgfbr2* knockout mice; Dr. Hideki Nakamura, Dr. Tomohiko Wakayama, and Dr. Shoichi Iseki for their technical advice concerning electron microscopic analysis; Dr. Hiroyuki Nishimura for critical reading of the manuscript; Dr. Masashi Akiyama for discussion; Dr. Atsushi Hirao and Dr. Masako Ohmura for the use of the flow cytometer; Dr. Ken Natsuga and Ms. Kaori Sakai for sample identification; and Ms. Misa Suzuki, Ms. Megumi Sato, and Ms. Yuika Osaki for technical assistance. This study was supported by grants from the Japanese Ministry of Education, Culture, Sports, Science, and Technology (17689033, 19390293), the Uehara Memorial Foundation, the Kato Memorial Bioscience Foundation, and the Takeda Science Foundation to E.K.N.

Received: May 13, 2009
Revised: July 27, 2010
Accepted: October 23, 2010
Published: February 3, 2011

REFERENCES

Arnold, I., and Watt, F.M. (2001). c-Myc activation in transgenic mouse epidermis results in mobilization of stem cells and differentiation of their progeny. Curr. Biol. *11*, 558–568.

Barrandon, Y., and Green, H. (1987). Three clonal types of keratinocyte with different capacities for multiplication. Proc. Natl. Acad. Sci. USA *84*, 2302–2306.

Benitah, S.A., Frye, M., Glogauer, M., and Watt, F.M. (2005). Stem cell depletion through epidermal deletion of Rac1. Science *309*, 933–935.

Blanpain, C., and Fuchs, E. (2006). Epidermal stem cells of the skin. Annu. Rev. Cell Dev. Biol. *22*, 339–373.

Blanpain, C., Lowry, W.E., Geoghegan, A., Polak, L., and Fuchs, E. (2004). Self-renewal, multipotency, and the existence of two cell populations within an epithelial stem cell niche. Cell *118*, 635–648.

Cotsarelis, G. (2006). Epithelial stem cells: A folliculocentric view. J. Invest. Dermatol. *126*, 1459–1468.

Darling, T.N., Bauer, J.W., Hintner, H., and Yancey, K.B. (1997). Generalized atrophic benign epidermolysis bullosa. Adv. Dermatol. *13*, 87–119, , discussion 120.

Dowling, J., Yu, Q.C., and Fuchs, E. (1996). Beta4 integrin is required for hemidesmosome formation, cell adhesion and cell survival. J. Cell Biol. *134*, 559–572.

Georges-Labouesse, E., Messaddeq, N., Yehia, G., Cadalbert, L., Dierich, A., and Le Meur, M. (1996). Absence of integrin alpha 6 leads to epidermolysis bullosa and neonatal death in mice. Nat. Genet. *13*, 370–373.

Greco, V., Chen, T., Rendl, M., Schober, M., Pasolli, H.A., Stokes, N., Dela Cruz-Racelis, J., and Fuchs, E. (2009). A two-step mechanism for stem cell activation during hair regeneration. Cell Stem Cell *4*, 155–169.

Green, H. (1977). Terminal differentiation of cultured human epidermal cells. Cell *11*, 405–416.

Guasch, G., Schober, M., Pasolli, H.A., Conn, E.B., Polak, L., and Fuchs, E. (2007). Loss of TGFbeta signaling destabilizes homeostasis and promotes squamous cell carcinomas in stratified epithelia. Cancer Cell *12*, 313–327.

Hintner, H., and Wolff, K. (1982). Generalized atrophic benign epidermolysis bullosa. Arch. Dermatol. *118*, 375–384.

Hojiro, O. (1972). Fine structure of the mouse hair follicle. J. Electron Microsc. (Tokyo) *21*, 127–138.

Inomata, K., Aoto, T., Binh, N.T., Okamoto, N., Tanimura, S., Wakayama, T., Iseki, S., Hara, E., Masunaga, T., Shimizu, H., and Nishimura, E.K. (2009). Genotoxic stress abrogates renewal of melanocyte stem cells by triggering their differentiation. Cell *137*, 1088–1099.

Iwata, H., Kamio, N., Aoyama, Y., Yamamoto, Y., Hirako, Y., Owaribe, K., and Kitajima, Y. (2009). IgG from patients with bullous pemphigoid depletes cultured keratinocytes of the 180-kDa bullous pemphigoid antigen (type XVII collagen) and weakens cell attachment. J. Invest. Dermatol. *129*, 919–926.

Leatherman, J.L., and Dinardo, S. (2010). Germline self-renewal requires cyst stem cells and stat regulates niche adhesion in *Drosophila* testes. Nat. Cell Biol. *12*, 806–811.

Li, L., and Xie, T. (2005). Stem cell niche: Structure and function. Annu. Rev. Cell Dev. Biol. *21*, 605–631.

Mackenzie, M.A., Jordan, S.A., Budd, P.S., and Jackson, I.J. (1997). Activation of the receptor tyrosine kinase Kit is required for the proliferation of melanoblasts in the mouse embryo. Dev. Biol. *192*, 99–107.

Masunaga, T., Shimizu, H., Yee, C., Borradori, L., Lazarova, Z., Nishikawa, T., and Yancey, K.B. (1997). The extracellular domain of BPAG2 localizes to anchoring filaments and its carboxyl terminus extends to the lamina densa of normal human epidermal basement membrane. J. Invest. Dermatol. *109*, 200–206.

McGrath, J.A., Gatalica, B., Christiano, A.M., Li, K., Owaribe, K., McMillan, J.R., Eady, R.A., and Uitto, J. (1995). Mutations in the 180-kD bullous pemphigoid antigen (BPAG2), a hemidesmosomal transmembrane collagen (COL17A1), in generalized atrophic benign epidermolysis bullosa. Nat. Genet. *11*, 83–86.

McMillan, J.R., Akiyama, M., and Shimizu, H. (2003). Epidermal basement membrane zone components: Ultrastructural distribution and molecular interactions. J. Dermatol. Sci. *31*, 169–177.

Méndez-Ferrer, S., Michurina, T.V., Ferraro, F., Mazloom, A.R., Macarthur, B.D., Lira, S.A., Scadden, D.T., Ma'ayan, A., Enikolopov, G.N., and Frenette, P.S. (2010). Mesenchymal and haematopoietic stem cells form a unique bone marrow niche. Nature *466*, 829–834.

Moore, K.A., and Lemischka, I.R. (2006). Stem cells and their niches. Science *311*, 1880–1885.

Morris, R.J., Liu, Y., Marles, L., Yang, Z., Trempus, C., Li, S., Lin, J.S., Sawicki, J.A., and Cotsarelis, G. (2004). Capturing and profiling adult hair follicle stem cells. Nat. Biotechnol. *22*, 411–417.

Nishie, W., Sawamura, D., Goto, M., Ito, K., Shibaki, A., McMillan, J.R., Sakai, K., Nakamura, H., Olasz, E., Yancey, K.B., et al. (2007). Humanization of autoantigen. Nat. Med. *13*, 378–383.

Nishimura, E.K., Yoshida, H., Kunisada, T., and Nishikawa, S.I. (1999). Regulation of E- and P-cadherin expression correlated with melanocyte migration and diversification. Dev. Biol. *215*, 155–166.

Nishimura, E.K., Jordan, S.A., Oshima, H., Yoshida, H., Osawa, M., Moriyama, M., Jackson, I.J., Barrandon, Y., Miyachi, Y., and Nishikawa, S. (2002). Dominant role of the niche in melanocyte stem-cell fate determination. Nature *416*, 854–860.

Nishimura, E.K., Granter, S.R., and Fisher, D.E. (2005). Mechanisms of hair graying: Incomplete melanocyte stem cell maintenance in the niche. Science *307*, 720–724.

Nishimura, E.K., Suzuki, M., Igras, V., Du, J., Lonning, S., Miyachi, Y., Roes, J., Beermann, F., and Fisher, D.E. (2010). Key roles for transforming growth factor beta in melanocyte stem cell maintenance. Cell Stem Cell *6*, 130–140.

Nishizawa, Y., Uematsu, J., and Owaribe, K. (1993). HD4, a 180 kDa bullous pemphigoid antigen, is a major transmembrane glycoprotein of the hemidesmosome. J. Biochem. *113*, 493–501.

Nowak, J.A., Polak, L., Pasolli, H.A., and Fuchs, E. (2008). Hair follicle stem cells are specified and function in early skin morphogenesis. Cell Stem Cell *3*, 33–43.

Olasz, E.B., Roh, J., Yee, C.L., Arita, K., Akiyama, M., Shimizu, H., Vogel, J.C., and Yancey, K.B. (2007). Human bullous pemphigoid antigen 2 transgenic skin elicits specific IgG in wild-type mice. J. Invest. Dermatol. *127*, 2807–2817.

Omatsu, Y., Sugiyama, T., Kohara, H., Kondoh, G., Fujii, N., Kohno, K., and Nagasawa, T. (2010). The essential functions of adipo-osteogenic progenitors as the hematopoietic stem and progenitor cell niche. Immunity *33*, 387–399.

Osawa, M., Egawa, G., Mak, S.S., Moriyama, M., Freter, R., Yonetani, S., Beermann, F., and Nishikawa, S. (2005). Molecular characterization of melanocyte stem cells in their niche. Development *132*, 5589–5599.

Oshima, M., Oshima, H., and Taketo, M.M. (1996). TGF-beta receptor type II deficiency results in defects of yolk sac hematopoiesis and vasculogenesis. Dev. Biol. *179*, 297–302.

Oshima, H., Rochat, A., Kedzia, C., Kobayashi, K., and Barrandon, Y. (2001). Morphogenesis and renewal of hair follicles from adult multipotent stem cells. Cell *104*, 233–245.

Paus, R., and Cotsarelis, G. (1999). The biology of hair follicles. N. Engl. J. Med. *341*, 491–497.

Paus, R., Müller-Röver, S., Van Der Veen, C., Maurer, M., Eichmüller, S., Ling, G., Hofmann, U., Foitzik, K., Mecklenburg, L., and Handjiski, B. (1999). A comprehensive guide for the recognition and classification of distinct stages of hair follicle morphogenesis. J. Invest. Dermatol. *113*, 523–532.

Powell, A.M., Sakuma-Oyama, Y., Oyama, N., and Black, M.M. (2005). Collagen XVII/BP180: a collagenous transmembrane protein and component of the dermoepidermal anchoring complex. Clin. Exp. Dermatol. *30*, 682–687.

Qiao, W., Li, A.G., Owens, P., Xu, X., Wang, X.J., and Deng, C.X. (2006). Hair follicle defects and squamous cell carcinoma formation in Smad4 conditional knockout mouse skin. Oncogene *25*, 207–217.

Raghavan, S., Bauer, C., Mundschau, G., Li, Q., and Fuchs, E. (2000). Conditional ablation of beta1 integrin in skin. Severe defects in epidermal proliferation, basement membrane formation, and hair follicle invagination. J. Cell Biol. *150*, 1149–1160.

Raymond, K., Deugnier, M.A., Faraldo, M.M., and Glukhova, M.A. (2009). Adhesion within the stem cell niches. Curr. Opin. Cell Biol. *21*, 623–629.

Tumbar, T., Guasch, G., Greco, V., Blanpain, C., Lowry, W.E., Rendl, M., and Fuchs, E. (2004). Defining the epithelial stem cell niche in skin. Science *303*, 359–363.

van der Neut, R., Krimpenfort, P., Calafat, J., Niessen, C.M., and Sonnenberg, A. (1996). Epithelial detachment due to absence of hemidesmosomes in integrin beta 4 null mice. Nat. Genet. *13*, 366–369.

Waikel, R.L., Kawachi, Y., Waikel, P.A., Wang, X.J., and Roop, D.R. (2001). Deregulated expression of c-Myc depletes epidermal stem cells. Nat. Genet. *28*, 165–168.

Watt, F.M. (2002). Role of integrins in regulating epidermal adhesion, growth and differentiation. EMBO J. *21*, 3919–3926.

Yang, L., Mao, C., Teng, Y., Li, W., Zhang, J., Cheng, X., Li, X., Han, X., Xia, Z., Deng, H., and Yang, X. (2005). Targeted disruption of Smad4 in mouse epidermis results in failure of hair follicle cycling and formation of skin tumors. Cancer Res. *65*, 8671–8678.

Yang, L., Wang, L., and Yang, X. (2009). Disruption of Smad4 in mouse epidermis leads to depletion of follicle stem cells. Mol. Biol. Cell *20*, 882–890.

Zanet, J., Pibre, S., Jacquet, C., Ramirez, A., de Alborán, I.M., and Gandarillas, A. (2005). Endogenous Myc controls mammalian epidermal cell size, hyperproliferation, endoreplication and stem cell amplification. J. Cell Sci. *118*, 1693–1704.

Hair Shaft Abnormalities in Localized Autosomal Recessive Hypotrichosis 2 and A Review of Other Non-syndromic Human Alopecias

Hiraku Suga[1], Yuichiro Tsunemi[1], Makoto Sugaya[1], Satoru Shinkuma[2], Masashi Akiyama[2], Hiroshi Shimizu[2] and Shinichi Sato[1]
Departments of Dermatology, [1]Faculty of Medicine, University of Tokyo, 7-3-1 Hongo, Bunkyo-ku, Tokyo 113-8655, and [2]Hokkaido University Graduate School of Medicine, Sapporo, Japan. E-mail: hiraku_s2002@yahoo.co.jp
Accepted December 16, 2010.

Localized autosomal recessive hypotrichosis (LAH) 2 is a type of non-syndromic human alopecia that is inherited as an autosomal recessive trait. We describe here a patient with LAH2 who had mutations in the *lipase H* (*LIPH*) gene. We analysed hair shaft morphology using light and scanning electron microscopy (SEM). In addition, we review the features of other non-syndromic human alopecias.

CASE REPORT

The patient was a 4-year-old boy, the firstborn of healthy and unrelated Japanese parents, born after an uneventful pregnancy. He had scant hair at birth, which grew very slowly in infancy.

Clinical examination revealed hypotrichosis of the scalp (Fig. 1a). The hairs were sparse, thin, and curly, and not easily plucked. The left eyebrow hair was sparse, but the eyelashes and other body hair were present in normal amounts. Teeth, nails, and the ability to sweat were completely normal. Clinical features of keratosis pilaris, milia, scarring, and palmoplantar keratoderma were absent. Psychomotor development was normal. The patient's younger brother also had severe hypotrichosis; since birth his hair was curly, and his eyebrow hair virtually absent (Fig. 1b). No other family members, including his parents, had similar hair abnormalities. Laboratory tests of the patient showed normal serum levels of copper and zinc, and liver and kidney function tests were all within normal ranges. Over a period of 2 years there was no improvement or exacerbation of hypotrichosis in the patient.

Light microscopy of the patient's scalp hairs revealed that approximately 10% had structural abnormalities. Abnormal hairs were composed of thick dark parts and thin light parts (Fig. 2a). SEM revealed alterations of the cuticular architecture. Cuticular cells were absent from both the thick and thin parts (Fig. 2b). Cross-sectional observation showed that thick, but not thin, sections had hair medulla (Fig. 2c, d). Light microscopy on hairs from the patient's younger brother revealed that they were composed of thin and thick parts (data not shown).

Based on the clinical features, hair microscopy and family pedigree, we suspected LAH2 or LAH3. To determine the type of LAH, we looked for gene mutations in *LIPH* and *LPAR6* (encoding lysophosphatidic acid receptor 6). Two prevalent missense mutations in *LIPH* were found (1); c.736T>A (p.Cys246Ser) and c.742C>A (p.His248Asn). The mutations were carried in a compound heterozygous state. No mutations were found in *LPAR6*. The parents did not consent to genetic testing of the younger brother or themselves.

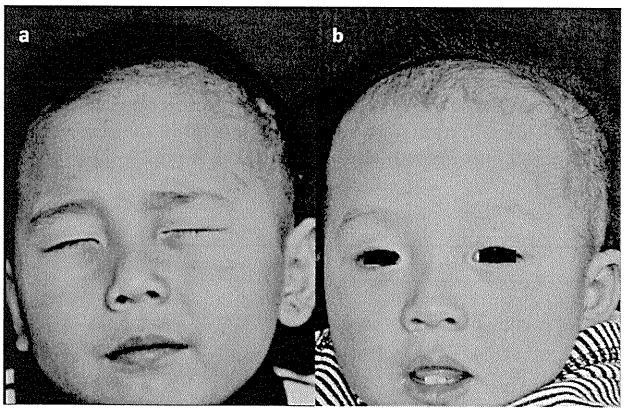

Fig. 1. (a) Clinical features of the patient at 4 years of age. (b) Clinical features of the younger brother at 1 year 4 months of age. Permission is given from the parents to publish these photos.

DISCUSSION

The different LAH subtypes map to chromosomes 18q12.1, 3q27.3 and 13q14.11–13q21.32, and are designated LAH1, LAH2 and LAH3, respectively (2–4). Mutations in *DSG4* (encoding desmoglein 4) have been found to be responsible for LAH1 (5). Kazantseva et al. (6) reported deletion mutations in *LIPH* leading to LAH2. Pasternack et al. (7) reported disruption of *LPAR6* in families affected with LAH3.

Table I summarizes of genetic, non-syndromic human alopecias. In *hypotrichosis simplex of the scalp*, hair loss

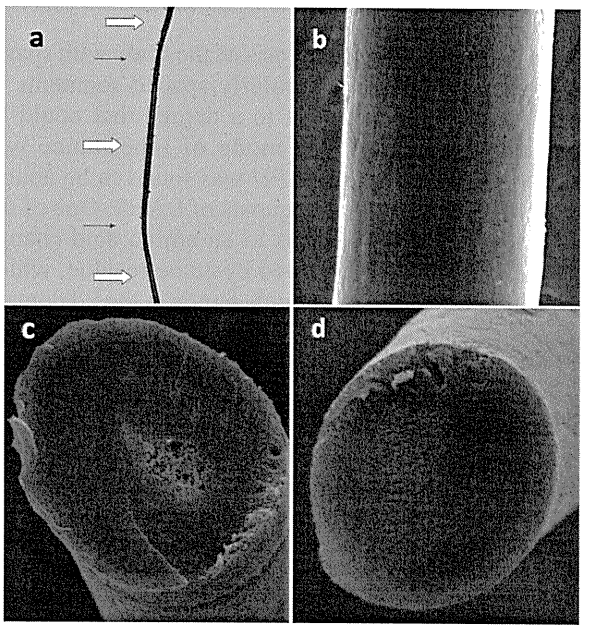

Fig. 2. (a) Light microscopy (×40). Hair was composed of thick (⇨) and thin parts (→). (b) Scanning electron microscopy (×900). Cuticular cells were absent in both thick and thin sections. (c, d) Scanning electron microscopy (cross-section, ×900). (c) Thick regions showed hair medulla, while (d) thin regions did not.

is limited to the scalp without hair shaft abnormalities. The causative gene is *CDSN* (encoding corneodesmosin) on 6p21.3 (8). The clinical presentations of *monilethrix* vary among patients. Mild cases have hair loss limited to the scalp, while severe cases show generalized alopecia. Hair shaft abnormalities are characteristic, demonstrating regularly-spaced, spindle-shaped swellings. The nodes are as thick as normal hair and the atrophic internodes represent areas where the hair is easily broken. Causative genes are *hHb1*, *hHb3* and *hHb6* (12q13) (9), which encode for basic hair keratins.

In case of *atrichia with papular lesions*, hair loss on the entire body occurs several months after birth. The gene responsible is *HR* (encoding "hairless") (10), a transcription modulating factor that influences the regression phase of the hair shaft cycle. Patients with *hypotrichosis, Marie Unna type* have hard and rough scalp hair, described as iron-wire hair. Generalized hypotrichosis is often seen. *U2HR*, an inhibitory upstream open reading frame of the human hairless gene (11), is mutated in this condition. *Hereditary hypotrichosis simplex* is characterized by hair follicle miniaturization. The defective gene is *APCDD1* (encoding adenomatosis polyposis down-regulated 1) (12). Hairs are short, thin, and easily plucked. Eyelashes and eyebrows are also affected.

As already mentioned, there are three types of *localized hereditary hypotrichosis*. LAH1 patients have hair shaft abnormalities that resemble moniliform hair (13). LAH1 can be viewed as an autosomal recessive form of monilethrix. Patients with LAH2 and LAH3 have woolly hair (14, 15), and eyelashes and eyebrows are often sparse or absent. Upper and lower limb hairs are sometimes absent too.

Our patient had hypotrichosis of the scalp with sparse left eyebrow hair and irregularly spaced segments of thick and thin hair, but not to a degree that could be labelled moniliform. The mode of inheritance was autosomal recessive and *LIPH* was found to be abnormal, thus establishing a diagnosis of LAH2. One of the mutations (c.736T>A) leads to an amino acid change (p.Cys246Ser) of a conserved cysteine residue, which forms intramolecular disulphide bonds in the lid domain in the structure model of LIPH (1). The other mutation (c.742C>A) results in alteration of one of the amino acids of the catalytic triad (Ser^{154}, Asp^{178}, and His^{248}) of LIPH (p.His248Asn) (1).

Regarding hair shaft morphology, Horev et al. (14) reported that hairs of LAH2 patients showed decreased diameter under light microscopy. This is the first report to describe hairs from an LAH2 patient by SEM. Shimomura et al. (13) observed hairs of LAH1 patients by SEM and found variable thickness of the hair shaft, resulting in nodes and internodes. Which are absent in LAH1 (our observation). Longitudinal ridges and flutes were observed at internodes, and the breaks always occurred at internodes in LAH1. These features resemble those of moniliform hair rather than LAH2. However, in the end gene analysis is probably easier to accomplish than SEM to distinguish the two types of LAH.

ACNOWLEDGEMENTS

We thank Dr Andrew Blauvelt, Department of Dermatology, Oregon Health & Science University, for many helpful comments.

REFERENCES

1. Shinkuma S, Akiyama M, Inoue A, Aoki J, Natsuga K, Nomura T, et al. LIPH prevalent founder mutations lead to loss of P2Y5 activation ability of PA-PLA1α in autosomal recessive hypotrichosis. Hum Mutat 2010; 31: 602–610.
2. Rafique MA, Ansar M, Jamai SM, Malik S, Sohail M, Faiyaz-Ul-Haque M, et al. A locus for hereditary hypotrichosis localized to human chromosome 18q21.1. Eur J Hum Genet 2003; 11: 623–628.
3. Aslam M, Chahrour MH, Razzaq A, Haque S, Yan K, Leal SM, et al. A novel locus for autosomal recessive form of hypotrichosis maps to chromosome 3q26.33-q27.3. J Med Genet 2004; 41: 849–852.
4. Wali A, Chishti MS, Ayub M, Yasinzai M, Kafaitullah, Ali G, et al. Localization of a novel autosomal recessive hypotrichosis locus (LAH3) to chromosome 13q14.11-q21.32. Clin Genet 2007; 72: 23–29.
5. Kljuic A, Bazzi H, Sundberg JP, Martinez-Mir A, O'Shaughnessy R, Mahoney MG, et al. Desmoglein 4 in hair follicle differentiation and epidermal adhesion: evidence from inherited hypotrichosis and acquired pemphigus vulgaris. Cell 2003; 113: 249–260.
6. Kazantseva A, Goltsov A, Zinchenko R, Grigorenko AP, Abrukova AV, Moliaka YK, et al. Human hair growth deficiency is linked to a genetic defect in the phospholipase gene LIPH. Science 2006; 314: 982–985.
7. Pasternack SM, von Kugelgen I, Aboud KA, Lee YA, Ruschendorf F, Voss K, et al. G protein-coupled receptor P2RY5 and its ligand LPA are involved in maintenance of human hair growth. Nat Genet 2008; 40: 329–334.

Table I. *Features of genetic, non-syndromic human alopecias*

Disease (ref)	Hair shaft shape	Eyelash/eyebrow	Causative gene	Mode of inheritance
Hypotrichosis simplex of scalp (8)	Normal	Normal	*CDSN*	Autosomal dominant
Monilethrix (9)	Regularly spaced, spindle-shaped swellings	Absent to normal	*hHb1, 3, 6*	Autosomal dominant
Atrichia with papular lesions (10)	Normal	Absent	*HR*	Autosomal recessive
Hypotrichosis, Marie Unna type (11)	Iron-wire	Sparse	*U2HR*	Autosomal dominant
Hereditary hypotrichosis simplex (12)	Short, thin, easily plucked	Absent to sparse	*APCDD1*	Autosomal dominant
Localized hereditary hypotrichosis (LAH1) (2, 5, 13)	Moniliform	Absent to normal	*DSG4*	Autosomal recessive
Localized hereditary hypotrichosis (LAH2) (3, 6, 14)	Curled	Absent to normal	*LIPH*	Autosomal recessive
Localized hereditary hypotrichosis (LAH3) (4, 7, 15)	Curled	Absent to normal	*LPAR6*	Autosomal recessive

8. Davalos NO, Garicia-Vargas A, Pforr J, Davalos IP, Picos-Cardenas VJ, Garcia-Cruz D, et al. A non-sense mutation in the corneodesmosin gene in a Mexican family with hypotrichosis simplex of the scalp. Br J Dermatol 2005; 153: 1216–1219.
9. Richard G, Itin P, Lin JP, Bon A, Bale SJ. Evidence for genetic heterogeneity in monilethrix. J Invest Dermatol 1996; 107: 812–814.
10. Ahmad W, Faiyaz ul Haque M, Brancolini V, Tsou HC, ul Haque S, Lam H, et al. Alopecia universalis associated with a mutation in the human hairless gene. Science 1998; 279: 720–724.
11. Wen Y, Liu Y, Xu Y, Zhao Y, Hua R, Wang K, et al. Loss-of-function mutations of an inhibitory upstream ORF in the human hairless transcript cause Marie Unna hereditary hypotrichosis. Nat Genet 2009; 41: 228–233.
12. Shimomura Y, Agalliu D, Vonica A, Luria V, Wajid M, Baumer A, et al. APCDD1 is a novel Wnt inhibitor mutated in hereditary hypotrichosis simplex. Nature 2010; 464: 1043–1047.
13. Shimomura Y, Sakamoto F, Kariya N, Matsunaga K, Ito M. Mutations in the desmoglein 4 gene are associated with monilethrix-like congenital hypotrichosis. J Invest Dermatol 2006; 126: 1281–1285.
14. Horev L, Tosti A, Rosen I, Hershko K, Vincenzi C, Nanova K, et al. Mutations in lipase H cause autosomal recessive hypotrichosis simplex with wooly hair. J Am Acad Dermatol 2009; 61: 813–818.
15. Horev L, Saad-Edin B, Ingber A, Zlotogorski A. A novel deletion mutation in P2RY5/LPA_6 gene cause autosomal recessive woolly hair with hypotrichosis. J Eur Acad Dermatol Venereol 2010; 24: 858–859.

Clinics in Dermatology (2011) **29**, 412–419

ELSEVIER

Clinics in Dermatology

Ultrastructure and molecular pathogenesis of epidermolysis bullosa

Satoru Shinkuma, MD[a,*], James R. McMillan, MSc[b], Hiroshi Shimizu, MD[a]

[a]*Department of Dermatology, Hokkaido University Graduate School of Medicine, N15 W7, Sapporo 060-8638, Japan*
[b]*Centre for Children's Burns and Trauma Research, Queensland Children's Medical Research Institute, The University of Queensland, Brisbane, Queensland 4029, Australia*

Abstract Epidermolysis bullosa (EB) is classified into the three major subtypes depending on the level of skin cleavage within the epidermal keratinocyte or basement membrane zone. Tissue separation occurs within the intraepidermal cytoplasm of the basal keratinocyte, through the lamina lucida, or in sublamina densa regions of the basal lamina (basement membrane) in EB simplex, junctional EB, and dystrophic EB, respectively. Transmission electron microscopy (TEM) is an effective method for determining the level of tissue separation and hemidesmosome (HD) and anchoring fibril morphology if performed by experienced operators, and has proven to be a powerful technique for the diagnosis of new EB patients. Recent advances in genetic and immunofluorescence studies have enabled us to diagnose EB more easily and with greater accuracy. This contribution reviews TEM findings in the EB subtypes and discusses the importance of observations in the molecular morphology of HD and basement membrane associated structures.

Introduction

Epidermolysis bullosa (EB) comprises a group of hereditary disorders characterized by mechanical stress-induced blistering of the skin and mucous membranes.[1] This group of diseases is caused by a genetic abnormality in a single gene encoding one of 13 proteins involved in epidermal keratinocyte-basement membrane zone (BMZ) adhesion (Figure 1).[2,3] EB has typically been classified into three main subtypes, depending on the level of epidermal separation from the underlying basal lamina. Tissue separation occurs within the intraepidermal keratinocyte cytoplasm, through the lamina lucida, or in the sublamina densa in EB simplex (EBS), junctional EB (JEB), and dystrophic EB (DEB), respectively (Figure 2).[1] After the initial diagnosis based on careful examination of the clinical manifestations and inheritance pattern, a skin biopsy from a recently formed blister lesion should be taken to determine the level of tissue separation to classify the disease.[4]

Transmission electron microscopy (TEM) and immunofluorescence (IF) are both effective at determining the level of tissue separation.[5] Currently, IF is becoming increasingly important in the diagnosis of EB because TEM requires expensive equipment and significant experience and expertise to process skin biopsy specimens and accurately interpret the resulting micrographs.[4] The primary advantage of TEM, however, is that it can visualize ultrastructural abnormalities and provide a semiquantitative assessment of specific BMZ structural deficits.[6] Therefore TEM is likely to continue to assume an important role in both the clinical and research

* Corresponding author. Tel.: +81 11 716 1161x5962; fax: +81 11 706 7820l.
E-mail address: qxfjc346@ybb.ne.jp (S. Shinkuma).

0738-081X/$ – see front matter © 2011 Elsevier Inc. All rights reserved.
doi:10.1016/j.clindermatol.2011.01.010

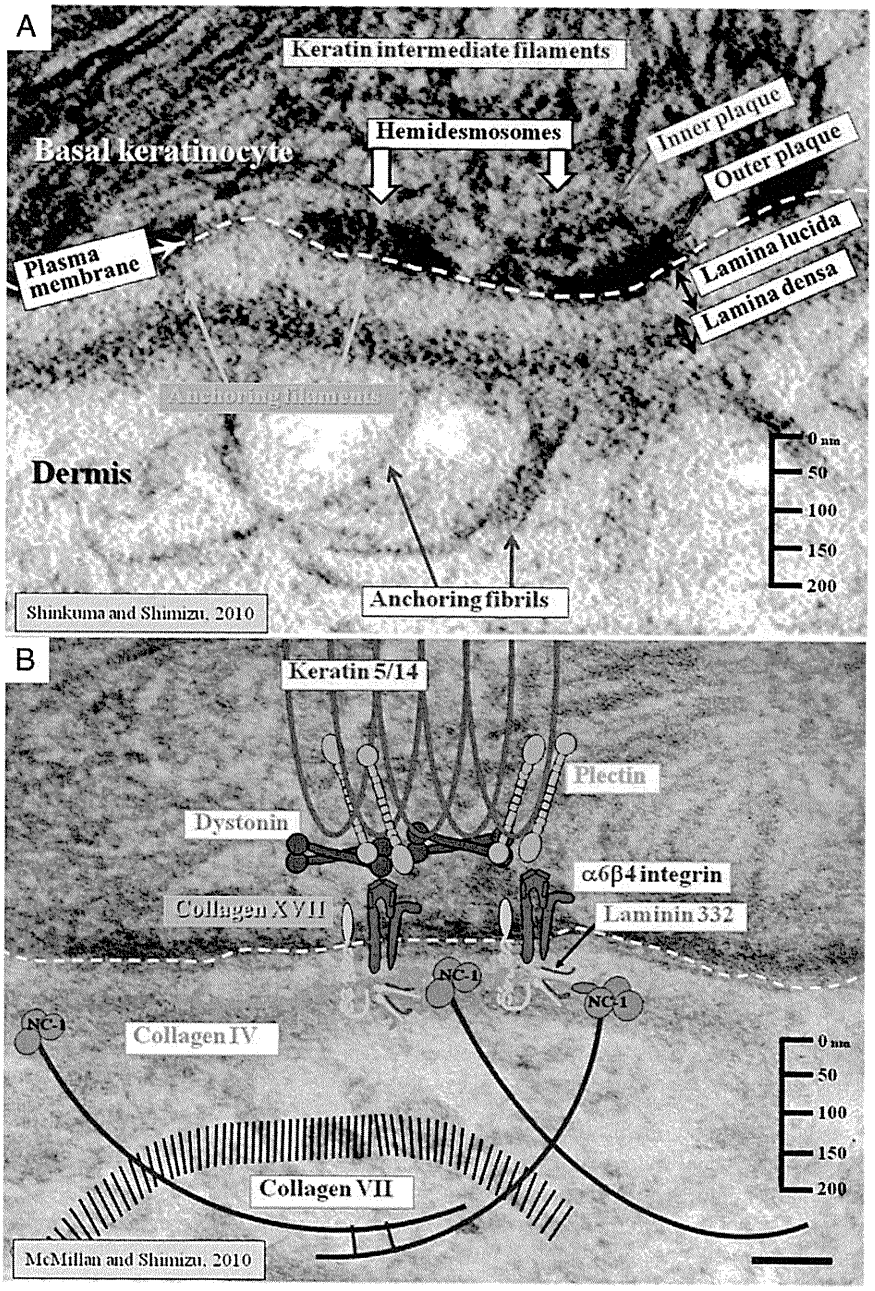

Fig. 1 Schematic diagram shows the approximate positions of principal epidermal basement membrane zone components. (Adapted with permission from McMillan et al.[3])

fields. This contribution focuses on TEM findings and their usefulness in EB diagnosis and cell adhesion research.

Ultrastructure of normal dermal–epidermal junction

The BMZ is composed of various molecules, each of which plays a differing role in dermal-epidermal junction adhesion (Figure 1).[3,7,8] The ultrastructural location of each BMZ molecule has been studied using a range of immunoelectron microscopy techniques.[7-9] In the basal keratinocyte, several electron dense rivetlike structures are found on the inner surface of the keratinocyte basal pole of the cell membrane, called hemidesmosomes (HDs).[10] HDs show a distinct tripartite, two-plaque structure, consisting of inner and outer plaques.[11-13] Keratin intermediate filaments (KIF), which are 10 to 12 mm thick and consist of basal cell keratins 5 and 14, associate with the inner hemidesmosome (HD) plaque and interplaque space and are capable of binding to both plectin and 230-kDa bullous pemphigoid

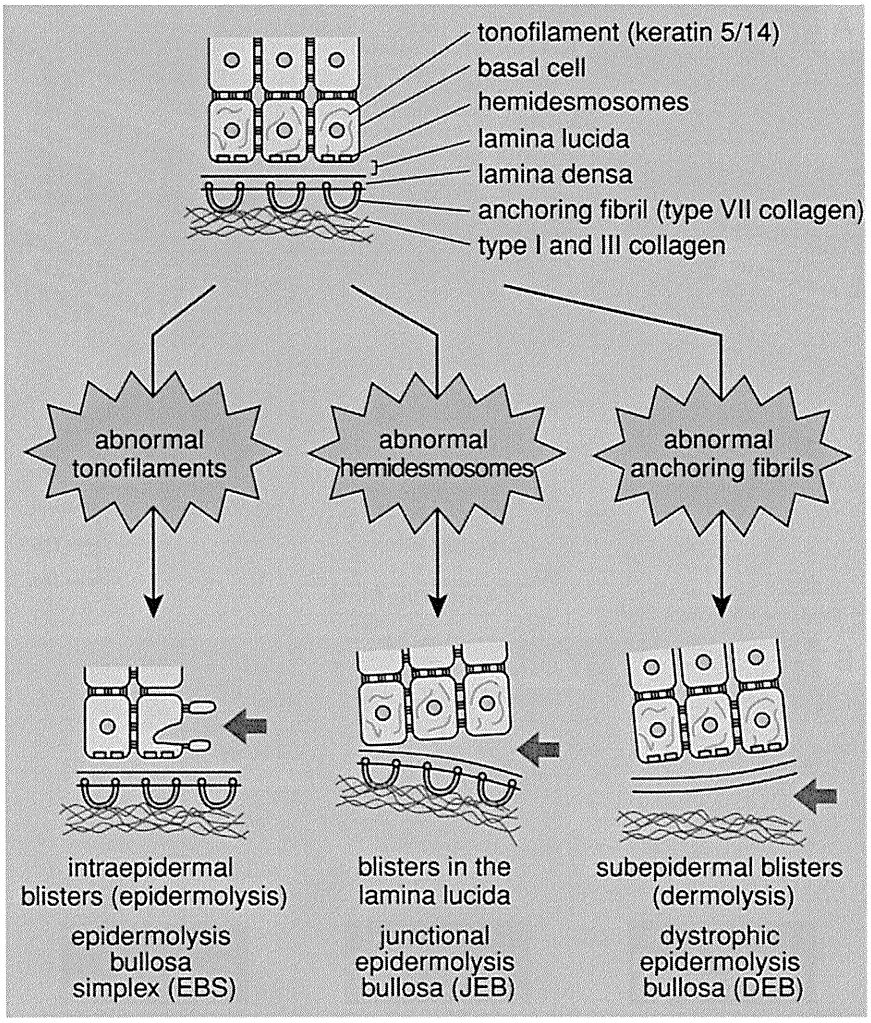

Fig. 2 The mechanism and the cleavage site of epidermolysis bullosa. (Adapted with permission from Shimizu H: Shimizu's Textbook of Dermatology: Blistering and Pustular Diseases. Sapporo, Japan: Hokkaido University Press/Nakayama Shoten Publishers. 2007:203p.).

antigen 1 (BPAG1e, BP230, also known as dystonin) hemidesmosomal antigens.[13-17] These two plakin protein family members, plectin and dystonin, form critical links in a continuous series of protein interactions bridging two distinct transmembrane molecular systems of the outer HD plaque, integrin $\alpha 6\beta 4$[18,19] and collagen XVII,[20,21] also known as 180-kDa bullous pemphigoid antigen 2 (BPAG2) or BP180.

Immediately beneath the keratinocyte plasma membrane lays an electron-lucent zone, the lamina lucida and an electron-dense layer comprising a closely packed fibrous network called the lamina densa.[7] Below the HD, there is a thin electron-dense line termed the subbasal dense plate, parallel to the plasma membrane that is visible in approximately one-third of HDs, depending on the precise orientation of the section.[10,22] Traversing the lamina lucida zone, subjacent to HDs, are thin anchoring filaments apparently inserting into the lamina densa. Laminin 332, one of the major epidermal laminins (formerly known as Kalinin, laminin 5), is found on the border between the upper lamina densa of HDs and lower lamina lucida at the base of anchoring filaments, which may comprise collagen XVII.[23,24] Beneath the lamina densa, most of the collagen VII molecules form semicircular loop structures called anchoring fibrils in which the amino (N-) terminals of the antiparallel collagen VII fibrils originate and terminate in the lamina densa.[3,25,26] In the dermis, anchoring fibrils may enable the lamina densa to link or encircle dermal collagen fibers or other components to provide basal lamina anchorage to the underlying structures.

Ultrastructural findings of EB

Epidermolysis bullosa simplex

The three major subtypes of EBS—Dowling-Meara (EBS-DM) (severe), other generalized (moderate), and the localized (mild) type—are caused by keratin 5 or 14 mutations that result in an abnormal keratin network leading

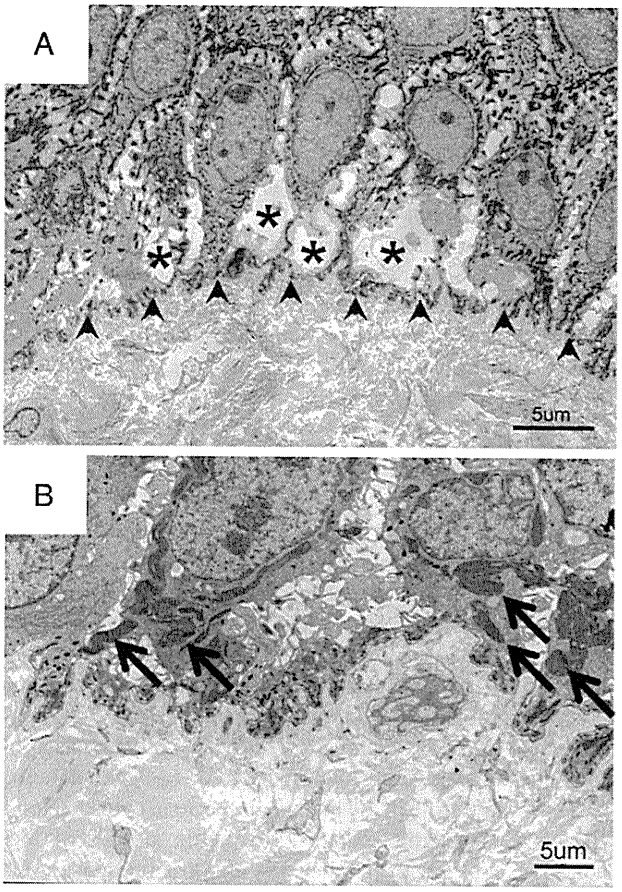

Fig. 3 Electron microscopic image of epidermolysis bullosa simplex shows (A) separation has occurred within the cytoplasm of the epidermal basal cells, which leads to intraepidermal blistering. The arrowheads indicate the lamina densa. The cytoplasm of the basal cells contains large vacuoles (asterisks) and show extensive damage. (B) Aggregation of keratin fibers is seen in epidermolysis bullosa simplex–Dowling-Meara (arrows).

to blister formation within the cytoplasm of the epidermal basal cells (Figure 3A).[27,28] In EBS-DM, in addition to the intraepidermal cleavage, clumping of degenerated keratin fibers can be observed within epidermal keratinocytes (Figure 3B).[29]

Rare types of EBS, including EBS with muscular dystrophy (EBS-MD) and EBS with pyloric atresia (EBS-PA), are caused by plectin gene mutations.[30-35] In EBS-MD and EBS-PA, the split occurs around the level of the HD inner plaque within the keratinocyte cytoplasm and is often associated with reduced numbers of poorly formed hypoplastic HDs, with reduced numbers of inner plaque and KIF association.[6,32]

Junctional EB

JEB can be further divided into three subtypes: Herlitz JEB, non-Herlitz JEB, and JEB with pyloric atresia.[1] All JEB subtypes are inherited in an autosomal-recessive manner and are characterized by blister formation in the lamina lucida.[36] Herlitz JEB, the most severe type, is caused by a complete absence of laminin 332.[37-39] Non-Herlitz JEB is caused by missense mutations leading to a reduction in functional laminin 332 or complete absence of collagen XVII.[37] JEB with pyloric atresia is caused by a genetic mutation in the integrin $\alpha 6$ or $\beta 4$ subunits that are the main receptor for ligand laminin 332 beneath HDs.[40,41]

Ultrastructurally, Herlitz JEB is characterized by widespread epidermal separation through the lamina lucida or by hypoplastic (small), or both, and a markedly reduced number of HDs (Figure 4).[6,22] In non-Herlitz JEB, HDs may appear normal or reduced in size or number.[6,42]

Dystrophic EB

DEB is caused by mutations in the gene that codes collagen VII, a major structural component of anchoring fibrils that is essential for connecting the dermis and the basal lamina and hence the epidermis.[3,9,43] Subepidermal blistering occurs in conjunction with reductions in anchoring fibril

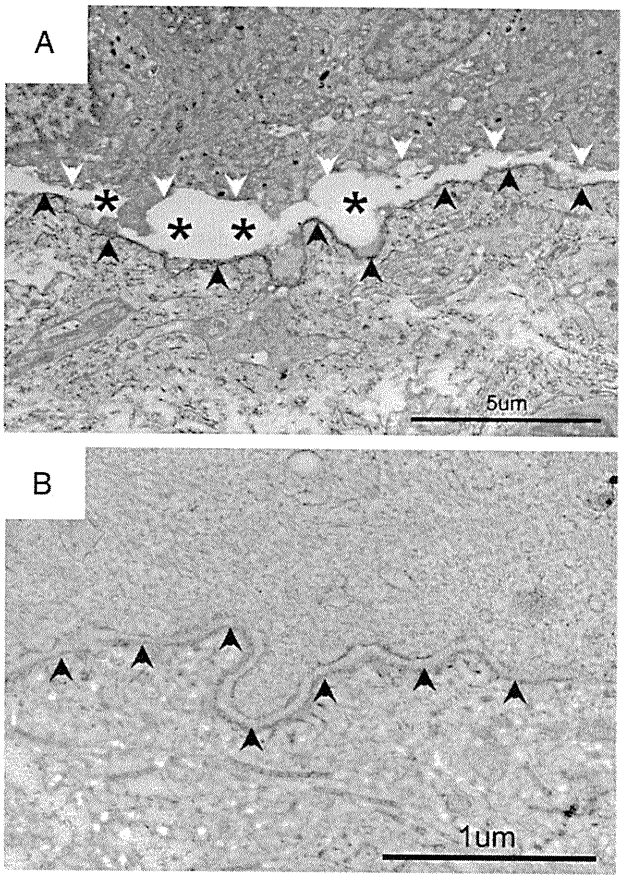

Fig. 4 Electron microscopic image of junctional epidermolysis bullosa (JEB) shows (A) a blister (asterisks) is present within the lamina lucida, between the plasma membrane of the basal keratinocytes (white arrowheads) and the lamina densa (black arrowheads). (B) The hemidesmosomes are rudimentary and reduced in number in Herlitz JEB.

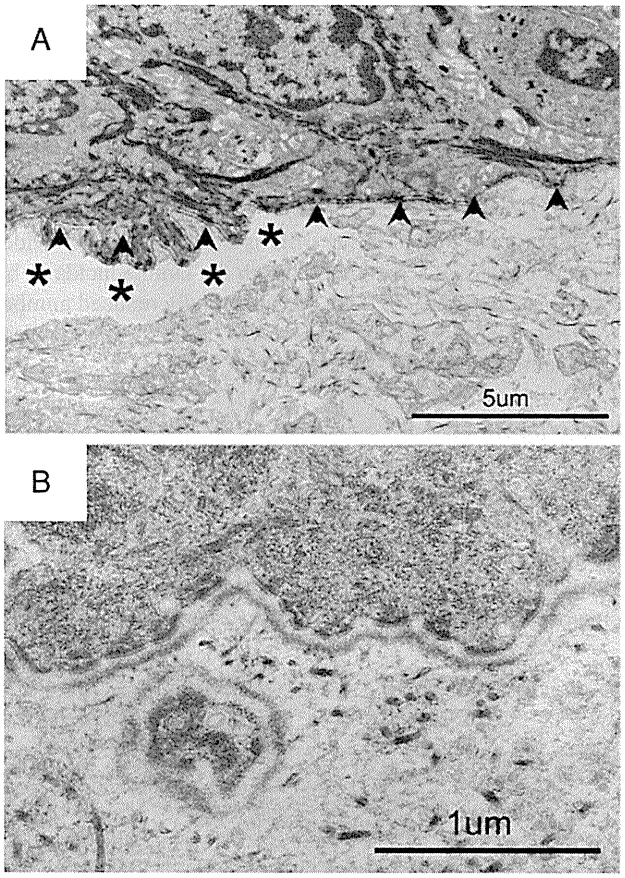

Fig. 5 Electron microscopic image of dystrophic epidermolysis bullosa shows (A) dissociation (asterisks) immediately below the lamina densa (arrowheads). (B) It is characterized by hypoplasia of anchoring fibrils.

numbers or with defects in normal anchoring fibril morphology, or both (Figure 5).[44] The phenotype of autosomal-dominant DEB (DDEB) is milder than that of recessive DEB (RDEB).[45] The most severe subtype of RDEB, severe generalized type, shows a severe reduction or lack of expression of collagen VII, which ultrastructurally results in rudimentary or absent anchoring fibrils (Figure 5).[44] By contrast, in the milder RDEB phenotype, termed "generalized other RDEB", shows reduced or rudimentary-appearing anchoring fibrils. In DDEB, anchoring fibrils are typically seen as normal in appearance or slightly decreased in number.

Kindler syndrome

Kindler syndrome has been added as a further, specific subtype of EB, in the latest classification of EB.[1,46] Kindler syndrome is inherited in an autosomal-recessive manner and is characterized by trauma-induced blistering, poikiloderma (skin atrophy and altered skin pigmentation), mucosal inflammation, and varying degrees of photosensitivity.[46] The pathogenesis of Kindler syndrome involves loss-of-function mutations in a newly recognized actin cytoskeleton-associated protein, now known as fermitin family homolog 1 and encoded by the gene *FERMT1*.[47] This protein has a role in controlling/activating β1 associated integrin cell adhesion and may play a role in the linkage of the actin cytoskeleton to β1 integrins and the extracellular matrix at sites of focal adhesion. Whereas EB is caused by abnormalities in HD-KIF cell attachment to the underlying basal lamina and dermis, Kindler syndrome is caused by defective activation of focal adhesion anchorage.[48] Ultrastructural examination of Kindler syndrome reveals a distinct disorganization below the

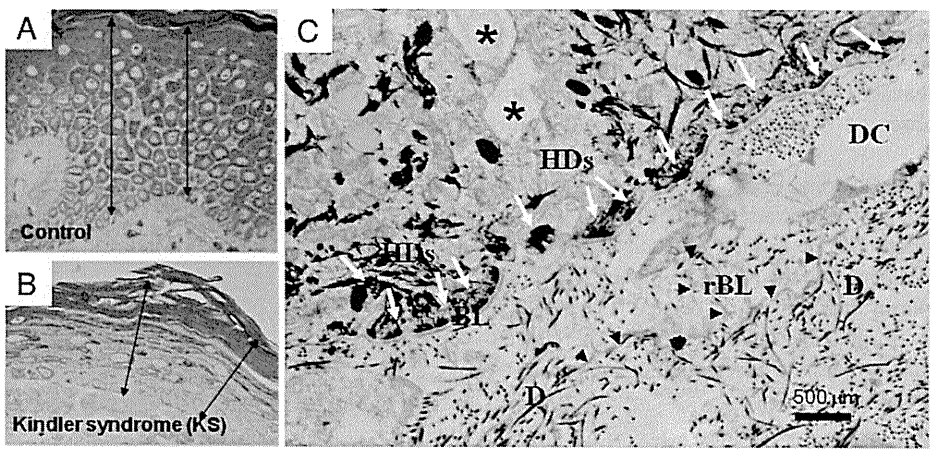

Fig. 6 Electron microscopic image of Kindler syndrome (KS) shows that (A) compared with the site-matched skin of healthy controls, (B) the skin of the KS patient has a thinner epidermis resulting from fewer cell layers. (C) Ultrastructurally, along the dermal-epidermal junction in the KS patient's skin, the hemidesmosomes (HDs) appear normal (white arrow); however, there may be signs of epidermal separation within the basal keratinocyte (asterisks) or immediately below the lamina densa as dermal clefts (DC). A common finding is the reduplication of the lamina densa (arrowheads) is seen in the upper dermis. Dermal cleft formation can occur together with reduplication of the lamina densa.

epidermal keratinocyte basement membrane exhibiting as lamina densa reduplication with branching, folding, and formation of loops and circles.[49] Cleft formation can occur at various sites along the dermal–epidermal junction, the largest and most common being below the lamina densa (Figure 6).[50] HDs and anchoring fibrils typically appear normal and with normal frequency, but there can be concomitant disturbances in the KIF network.

The role of electron microscopy in EB

Recent advances in genetic and IF techniques have enabled us to diagnose EB more rapidly and with greater accuracy regarding the particular underlying genetic defects.[1,2] We cannot, however, sufficiently predict precise clinical manifestations of each EB subtype using these techniques alone. Gene analysis cannot always precisely predict EB disease severity from novel mutations, although some successful genotype–phenotype correlations have been reported.[51,52] One reason is that most cases of JEB and RDEB are inherited in an autosomal-recessive manner and are thus caused by compound heterozygous gene mutations; therefore, it is usually difficult to assess the clinical phenotype and function of each mutant protein derived from different maternal or paternal mutations. Another reason is that there may exist, as yet undiscovered, modifier genes that influence EB disease severity, other than the causative gene.[53]

IF studies also have limited ability to assess disease severity by measuring the expression level of particular constitutive BMZ proteins, because the clinical severities of EBS, DDEB, and parts of autosomal-recessive EB with

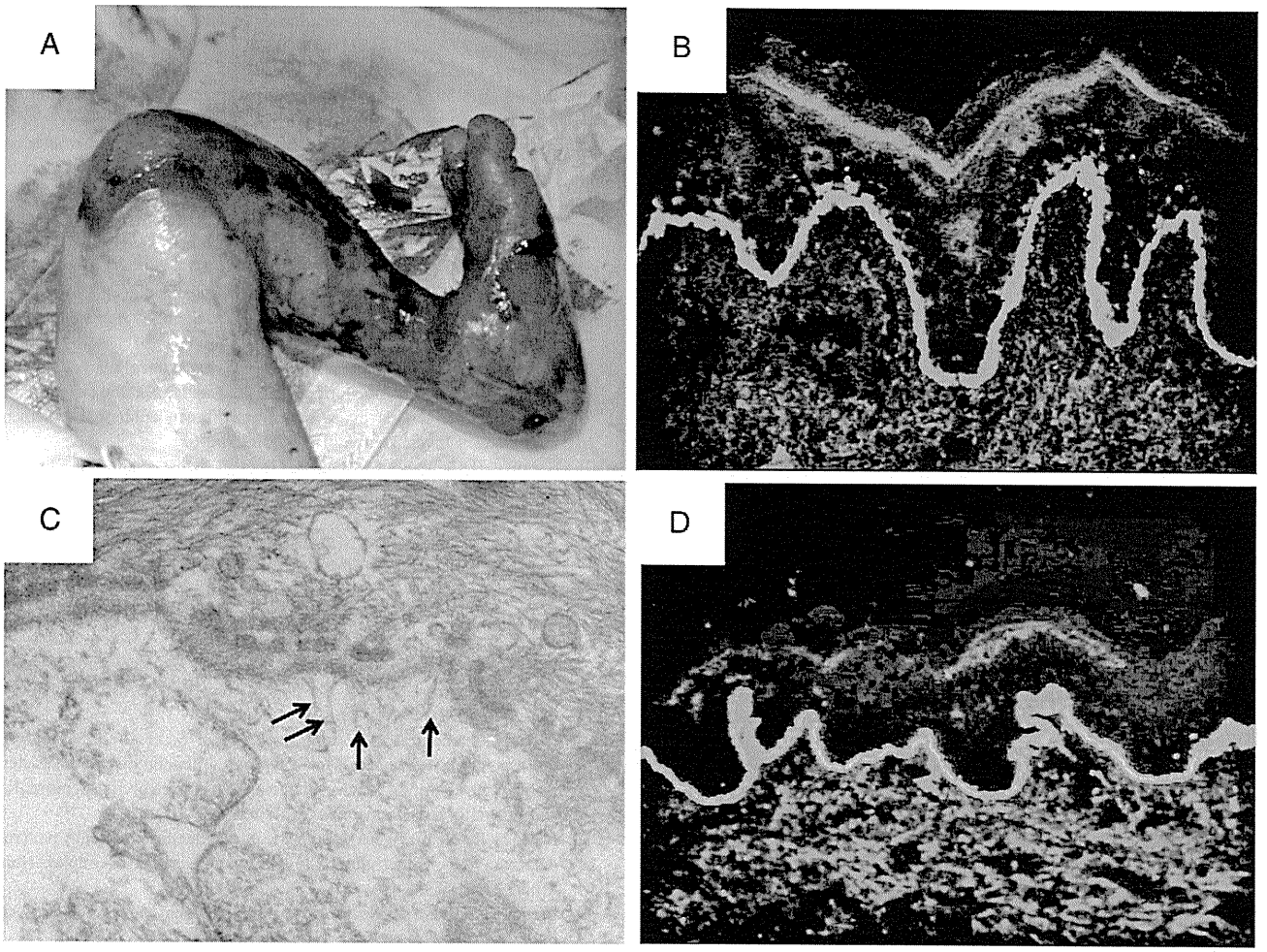

Fig. 7 A case of recessive dystrophic epidermolysis bullosa (EB) with missense mutation. (A) The patient exhibits a clinical severity similar to the most severe subtype of recessive dystrophic EB (DEB), the severe generalized type. (B) Immunofluorescence staining for collagen VII shows the expression level of collagen VII is just slightly reduced for the severe manifestation. (C) The electron micrograph of the DEB epidermal basement membrane zone. There are rudimentary-appearing anchoring fibrils, which are slightly reduced in number (arrow). (D) Normal control of immunofluorescence staining for collagen VII. In this case, the clinical severity correlates with the morphology of each mutant collagen VII anchoring fibril rather than the expression level.

missense mutations correlate with the combined function of the mutant proteins rather than the expression levels of both wild-type normal or abnormal protein expression examined by IF staining (Figure 7).[54] In these cases, determination of the precise molecular morphology of BMZ components provides important clues to predict their clinical severities, organ involvement, and overall patient prognosis. A careful ultrastructural examination can thus provide some estimate of EB clinical severity and disease progression, not only from a quantitative ultrastructural analysis but also from a morphologic examination. Taken together, we propose that electron microscopic evaluation remains an important technique acting as a bridge between genetic and immunohistologic tests and has the ability to provide extra diagnostic clues and subsequent beneficial practical and clinical information for EB patients and their health care providers.

Acknowledgments

Hideki Nakamura contributed to the transmission electron micrographs.

References

1. Fine J, Eady R, Bauer E, et al. The classification of inherited epidermolysis bullosa (EB): Report of the Third International Consensus Meeting on Diagnosis and Classification of EB. J Am Acad Dermatol 2008;58:931-50.
2. Uitto J, Richard G. Progress in epidermolysis bullosa: from eponyms to molecular genetic classification. Clin Dermatol 2005;23:33-40.
3. McMillan J, Akiyama M, Shimizu H. Epidermal basement membrane zone components: ultrastructural distribution and molecular interactions. J Dermatol Sci 2003;31:169-77.
4. Sawamura D, Nakano H, Matsuzaki Y. Overview of epidermolysis bullosa. J Dermatol 2010;37:214-9.
5. Hintner H, Stingl G, Schuler G, et al. Immunofluorescence mapping of antigenic determinants within the dermal-epidermal junction in the mechanobullous diseases. J Invest Dermatol 1981;76:113-8.
6. McMillan J, McGrath J, Tidman M, et al. Hemidesmosomes show abnormal association with the keratin filament network in junctional forms of epidermolysis bullosa. J Invest Dermatol 1998;110:132-7.
7. McMillan J, Akiyama M, Nakamura H, et al. Colocalization of multiple laminin isoforms predominantly beneath hemidesmosomes in the upper lamina densa of the epidermal basement membrane. J Histochem Cytochem 2006;54:109-18.
8. McMillan J, Long H, Akiyama M, et al. Epidermolysis bullosa: diagnosis and therapy. Wound Pract Res 2009;17:62-70.
9. Shimizu H. New insights into the immunoultrastructural organization of cutaneous basement membrane zone molecules. Exp Dermatol 1998;7:303-13.
10. Tidman M, Eady R. Ultrastructural morphometry of normal human dermal-epidermal junction. The influence of age, sex, and body region on laminar and nonlaminar components. J Invest Dermatol 1984;83:448-53.
11. Briggaman R, Wheeler CJ. The epidermal-dermal junction. J Invest Dermatol 1975;65:71-84.
12. Legan P, Collins J, Garrod D. The molecular biology of desmosomes and hemidesmosomes: "what's in a name"? Bioessays 1992;14:385-93.
13. McMillan J, Eady R. Hemidesmosome ontogeny in digit skin of the human fetus. Arch Dermatol Res 1996;288:91-7.
14. Ghohestani R, Li K, Rousselle P, et al. Molecular organization of the cutaneous basement membrane zone. Clin Dermatol 2001;19:551-62.
15. Wiche G. Role of plectin in cytoskeleton organization and dynamics. J Cell Sci 1998;111:2477-86.
16. Yang Y, Dowling J, Yu Q, et al. An essential cytoskeletal linker protein connecting actin microfilaments to intermediate filaments. Cell 1996;86:655-65.
17. Groves R, Liu L, Dopping-Hepenstal P, et al. A homozygous nonsense mutation within the dystonin gene coding for the coiled-coil domain of the epithelial isoform of BPAG1 underlies a new subtype of autosomal recessive epidermolysis bullosa simplex. J Invest Dermatol 2010;130:1551-7.
18. Niessen C, Cremona O, Daams H, et al. Expression of the integrin alpha 6 beta 4 in peripheral nerves: localization in Schwann and perineural cells and different variants of the beta 4 subunit. J Cell Sci 1994;107:543-52.
19. Niessen C, van der Raaij-Helmer M, Hulsman E, et al. Deficiency of the integrin beta 4 subunit in junctional epidermolysis bullosa with pyloric atresia: consequences for hemidesmosome formation and adhesion properties. J Cell Sci 1996;109:1695-706.
20. Koster J, Geerts D, Favre B, et al. Analysis of the interactions between BP180, BP230, plectin and the integrin alpha6beta4 important for hemidesmosome assembly. J Cell Sci 2003;116:387-99.
21. Borradori L, Sonnenberg A. Structure and function of hemidesmosomes: more than simple adhesion complexes. J Invest Dermatol 1999;112:411-8.
22. Tidman M, Eady R. Hemidesmosome heterogeneity in junctional epidermolysis bullosa revealed by morphometric analysis. J Invest Dermatol 1986;86:51-6.
23. Masunaga T, Shimizu H, Ishiko A, et al. Localization of laminin-5 in the epidermal basement membrane. J Histochem Cytochem 1996;44:1223-30.
24. Masunaga T, Shimizu H, Yee C, et al. The extracellular domain of BPAG2 localizes to anchoring filaments and its carboxyl terminus extends to the lamina densa of normal human epidermal basement membrane. J Invest Dermatol 1997;109:200-6.
25. Shimizu H, Ishiko A, Masunaga T, et al. Most anchoring fibrils in human skin originate and terminate in the lamina densa. Lab Invest 1997;76:753-63.
26. Sakai L, Keene D, Morris N, et al. Type VII collagen is a major structural component of anchoring fibrils. J Cell Biol 1986;103:1577-86.
27. Lane E, Rugg E, Navsaria H, et al. A mutation in the conserved helix termination peptide of keratin 5 in hereditary skin blistering. Nature 1992;356:244-6.
28. Irvine A, McLean W. Human keratin diseases: the increasing spectrum of disease and subtlety of the phenotype-genotype correlation. Br J Dermatol 1999;140:815-28.
29. Ishida-Yamamoto A, McGrath J, Chapman S, et al. Epidermolysis bullosa simplex (Dowling-Meara type) is a genetic disease characterized by an abnormal keratin-filament network involving keratins K5 and K14. J Invest Dermatol 1991;97:959-68.
30. Natsuga K, Nishie W, Akiyama M, et al. Plectin expression patterns determine two distinct subtypes of epidermolysis bullosa simplex. Hum Mutat 2010;31:308-16.
31. Pfendner E, Uitto J. Plectin gene mutations can cause epidermolysis bullosa with pyloric atresia. J Invest Dermatol 2005;124:111-5.
32. Nakamura H, Sawamura D, Goto M, et al. Epidermolysis bullosa simplex associated with pyloric atresia is a novel clinical subtype caused by mutations in the plectin gene (PLEC1). J Mol Diagn 2005;7:28-35.
33. McMillan J, Akiyama M, Rouan F, et al. Plectin defects in epidermolysis bullosa simplex with muscular dystrophy. Muscle Nerve 2007;35:24-35.

34. McLean W, Pulkkinen L, Smith F, et al. Loss of plectin causes epidermolysis bullosa with muscular dystrophy: cDNA cloning and genomic organization. Genes Dev 1996;10:1724-35.
35. Smith F, Eady R, Leigh I, et al. Plectin deficiency results in muscular dystrophy with epidermolysis bullosa. Nat Genet 1996;13:450-7.
36. Anton-Lamprecht I, Schnyder U. Ultrastructure of epidermolyses with junctional blister formation (author's transl). Dermatologica 1979;159: 377-82.
37. McGrath J, Kivirikko S, Ciatti S, et al. A homozygous nonsense mutation in the alpha 3 chain gene of laminin 5 (LAMA3) in Herlitz junctional epidermolysis bullosa: prenatal exclusion in a fetus at risk. Genomics 1995;29:282-4.
38. Pulkkinen L, Christiano A, Airenne T, et al. Mutations in the gamma 2 chain gene (LAMC2) of kalinin/laminin 5 in the junctional forms of epidermolysis bullosa. Nat Genet 1994;6:293-7.
39. Ashton G, Mellerio J, Dunnill M, et al. A recurrent laminin 5 mutation in British patients with lethal (Herlitz) junctional epidermolysis bullosa: evidence for a mutational hotspot rather than propagation of an ancestral allele. Br J Dermatol 1997;136:674-7.
40. Vidal F, Aberdam D, Miquel C, et al. Integrin beta 4 mutations associated with junctional epidermolysis bullosa with pyloric atresia. Nat Genet 1995;10:229-34.
41. Ruzzi L, Gagnoux-Palacios L, Pinola M, et al. A homozygous mutation in the integrin alpha6 gene in junctional epidermolysis bullosa with pyloric atresia. J Clin Invest 1997;99:2826-31.
42. McGrath J, Gatalica B, Christiano A, et al. Mutations in the 180-kD bullous pemphigoid antigen (BPAG2), a hemidesmosomal transmembrane collagen (COL17A1), in generalized atrophic benign epidermolysis bullosa. Nat Genet 1995;11:83-6.
43. Christiano A, Greenspan D, Hoffman G, et al. A missense mutation in type VII collagen in two affected siblings with recessive dystrophic epidermolysis bullosa. Nat Genet 1993;4:62-6.
44. Tidman M, Eady R. Evaluation of anchoring fibrils and other components of the dermal-epidermal junction in dystrophic epidermolysis bullosa by a quantitative ultrastructural technique. J Invest Dermatol 1985;84:374-7.
45. Christiano A, McGrath J, Tan K, et al. Glycine substitutions in the triple-helical region of type VII collagen result in a spectrum of dystrophic epidermolysis bullosa phenotypes and patterns of inheritance. Am J Hum Genet 1996;58:671-81.
46. Lai-Cheong J, McGrath J. Kindler syndrome. Dermatol Clin 2010;28: 119-24.
47. Jobard F, Bouadjar B, Caux F, et al. Identification of mutations in a new gene encoding a FERM family protein with a pleckstrin homology domain in Kindler syndrome. Hum Mol Genet 2003;12: 925-35.
48. Lai-Cheong J, Tanaka A, Hawche G, et al. Kindler syndrome: a focal adhesion genodermatosis. Br J Dermatol 2009;160:233-42.
49. D'Souza M, Kimble R, McMillan J. Kindler syndrome pathogenesis and fermitin family homologue 1 (kindlin-1) function. Dermatol Clin 2010;28:115-8.
50. Yasukawa K, Sato-Matsumura K, McMillan J, et al. Exclusion of COL7A1 mutation in Kindler syndrome. J Am Acad Dermatol 2002;46: 447-50.
51. Arin M, Grimberg G, Schumann H, et al. Identification of novel and known KRT5 and KRT14 mutations in 53 patients with epidermolysis bullosa simplex: correlation between genotype and phenotype. Br J Dermatol 2010;162:1365-9.
52. Dang N, Klingberg S, Marr P, et al. Review of collagen VII sequence variants found in Australasian patients with dystrophic epidermolysis bullosa reveals nine novel COL7A1 variants. J Dermatol Sci 2007;46: 169-78.
53. Titeux M, Pendaries V, Tonasso L, et al. A frequent functional SNP in the MMP1 promoter is associated with higher disease severity in recessive dystrophic epidermolysis bullosa. Hum Mutat 2008;29: 267-76.
54. Eady R, Dopping-Hepenstal P. Transmission electron microscopy for the diagnosis of epidermolysis bullosa. Dermatol Clin 2010;28:211-22, vii.

Japanese-Specific Filaggrin Gene Mutations in Japanese Patients Suffering from Atopic Eczema and Asthma

Journal of Investigative Dermatology (2010) **130,** 2834–2836; doi:10.1038/jid.2010.218; published online 5 August 2010

TO THE EDITOR

Mutations in *FLG*, the gene encoding profilaggrin/filaggrin, are the underlying cause of ichthyosis vulgaris (OMIM 146700) and an important predisposing factor for atopic eczema (AE) (Sandilands *et al.*, 2007). *FLG* mutations are also significantly associated with asthma with AE mainly in the European population (Rodríguez *et al.*, 2009; van den Oord and Sheikh, 2010). The presence of population-specific *FLG* mutations has been reported in both the European and Asian races (Nomura *et al.*, 2007; Sandilands *et al.*, 2007). To clarify whether *FLG* mutations are a predisposing factor for asthma in the non-European population, we initially studied 172 Japanese AE patients (mean age, 24.8 ± 9.1 years) and 134 unrelated Japanese control individuals (healthy volunteers; mean age, 27.9 ± 6.0 years). All AE patients had been diagnosed based on widely recognized diagnostic criteria (Hanifin and Rajka, 1980). The majority of AE patients and control individuals were identical to those in a previous study (Nemoto-Hasebe *et al.*, 2010). In this AE cohort, 73 AE patients (mean age, 25.4 ± 8.9 years) experienced complications with asthma. Furthermore, we studied another Japanese asthma cohort (137 patients; mean age, 58.2 ± 16.9 years). Patients were considered asthmatic based on the presence of recurrent episodes of ≥2 of the three symptoms (coughing, wheezing, or dyspnea) associated with demonstrable reversible airflow limitation, either spontaneously or with an inhaled short-acting β2-agonist and/or increased airway responsiveness to methacholine (Isada *et al.*, 2010). Fully informed consent was obtained from the participants or their legal guardians for this study. This study had been approved by the Ethical Committee at Hokkaido University Graduate School of Medicine and was conducted according to the Declaration of Helsinki Principles.

FLG mutation screening revealed that 27.4% of patients in our Japanese AE complicated with asthma case series carried one or more of the eight *FLG* mutations (combined minor allele frequency of 0.151, $n=146$) (Table 1). Conversely, 26.3% of Japanese AE patients without asthma carried one or more of the eight *FLG* mutations (combined minor allele frequency of 0.147, $n=198$). The *FLG* variants are also carried by 3.7% of Japanese control individuals (combined minor allele frequency of 0.019, $n=268$). We found that all compound heterozygous mutations were present in *trans* by observing transmission or haplotype analysis (Nomura *et al.*, 2007, 2008). There is a statistically significant association between the eight *FLG* mutations and AE with asthma, and between the eight *FLG* mutations and AE without asthma (Table 1). Moreover, AE complicated with asthma manifested in heterozygous carriers of *FLG* mutations with an odds ratio for AE and asthma of 9.74 (95% confidence interval 3.47–27.32), suggesting a relationship between *FLG* mutations and AE with asthma.

In the Japanese general asthma cohort, 8.0% of the asthma patients carried one or more of the eight *FLG* mutations (combined minor allele frequency of 0.04, $n=274$) (Table 2). Whereas, of the Japanese patients with asthma complicated by AE, 22.2% carried one or more of the *FLG* mutations (combined minor allele frequency of 0.11, $n=36$). In contrast, 5.9% of asthma patients without AE carried one or more of the *FLG* mutations (combined minor allele frequency of 0.03, $n=238$). There was a statistically significant association between the eight *FLG* mutations and asthma with AE (Table 2). There was no statistically significant association between the *FLG* mutations and entire asthma patients, nor between *FLG* mutations and asthma without AE. We cannot exclude the possibility that this lack of significant association is due to the small number of the patients included in this study. We used the same control set for both case-controlled studies. Thus, strictly speaking, there is no independent replication for the control group.

Recent meta-analysis revealed that *FLG* mutations are significantly associated with asthma in the European population and there are especially, strong effects observed for *FLG* mutations for the compound phenotype, asthma in addition to eczema (Rodríguez *et al.*, 2009; van den Oord and Sheikh, 2010). In contrast, there appeared to be no association of *FLG* mutations with asthma in the absence of eczema (Rodríguez *et al.*, 2009; van den Oord and Sheikh, 2010).

This Japanese cohort has a completely different *FLG* mutation spectrum from those in the European and the North American populations. However, our results clearly confirm the strong association of *FLG* mutations with our Japanese cohort of AE patients with asthma complications, and the association of *FLG* mutations and asthma patients with AE complications, for the first time outside Europe or North America. Conversely, this study showed no significant correlation between general asthma patients and *FLG* mutations, suggesting that atopic asthma patients associated with *FLG* mutations are a minority among general asthma patients. The frequency of heterozygous, compound heterozygous, and homozygous *FLG* mutation carriers

Abbreviation: AE, atopic eczema

Table 1. Atopic eczema case–control association analysis for *FLG* null variants in Japan

	R501X		3321delA		S1695X		Q1701X		S2554X		S2889X		S3296X		K4022X		Combined			
Genotype	Con	AE	Con	AE	Con	AE	Con	AE	Con	AE	Con	AE	Con	AE	Con	AE	Con	AE (total)	AE (asthma+)	AE (asthma−)
AA	134	172	133	163	133	172	134	169	133	162	132	152	134	166	134	169	129	126	53	73
Aa	0	0	1	9	1	0	0	3	1	10	2	20	0	6	0	3	5	41	18	23
aa	0	0	0	0	0	0	0	0	0	0	0	0	0	0	0	0	0	5[1]	2	3
Total	134	172	134	172	134	172	134	172	134	172	134	172	134	172	134	172	134	172	73	99

Abbreviations: AE, atopic eczema; CI, confidence interval; Con, healthy control; OR, odds ratio.
For combined genotype: AE+asthma, exact *P*-value of Pearson χ^2-test=1.909×10^{-6}, OR and 95% CI for dominant models (AA vs aX)=9.737 (3.473–27.322); AE−asthma, exact *P*-value of Pearson χ^2-test=7.189×10^{-7}, OR and 95% CI for dominant models (AA vs aX)=9.191 (3.383–24.938); all AE, exact *P*-value of Pearson χ^2-test=1.189×10^{-7}, OR and 95% CI for dominant models (AA vs aX)=9.416 (3.625–24.450).
[1]All the five patients were compound heterozygotes for minor alleles.

Table 2. Asthma case–control association analysis for *FLG* null variants in Japan

	R501X		3321delA		S1695X		Q1701X		S2554X		S2889X		S3296X		K4022X		Combined			
Genotype	Con	Asthma	Con	Asthma	Con	Asthma	Con	Asthma	Con	Asthma	Con	Asthma	Con	Asthma	Con	Asthma	Con	Asthma (total)	Asthma (AE+)	Asthma (AE−)
AA	134	137	133	137	133	137	134	137	133	133	132	132	134	136	134	136	129	126	14	112
Aa	0	0	1	0	1	0	0	0	1	4	2	5	0	1	0	1	5	11	4	7
aa	0	0	0	0	0	0	0	0	0	0	0	0	0	0	0	0	0	0	0	0
Total	134	137	134	137	134	137	134	137	134	137	134	137	134	137	134	137	134	137	18	119

Abbreviations: AE, atopic eczema; CI, confidence interval; Con, healthy control; OR, odds ratio.
For combined genotype: asthma+AE, exact *P*-value of Pearson χ^2-test=0.0122, OR and 95% CI for dominant models (AA vs aX)=7.3692 (1.7715–30.6748); asthma−AE, exact *P*-value of Pearson χ^2-test=0.5563, OR and 95% CI for dominant models (AA vs aX)=1.6124 (0.4979–5.2219); all asthma, exact *P*-value of Pearson χ^2-test=0.1968, OR and 95% CI for dominant models (AA vs aX)=2.2523 (0.7609–6.6667).

observed in our Japanese controls was only 3.7%, which was much lower than that seen in European general population, where it is approximately 7.5%. This suggested that there may be further mutations yet to be discovered in the Japanese. As we have sequenced more than 40 Japanese families with ichthyosis vulgaris, there is now little possibility that further highly prevalent mutations will be found in the Japanese population. However, it is still possible that there might be multiple, further low-frequency *FLG* mutations discovered in the Japanese population. In addition, because of the relatively small sample size of this genetic study, further replication in association studies will be required for *FLG* mutations and asthma in Japan.

In our cohorts, serum IgE levels were extremely high (median, 3141.9 IU ml^{-1}; 25th–75th percentiles, 1276.0–9753.0 IU ml^{-1}) in AE patients with asthma ($n=73$) in the AE cohort, compared with that in total asthma patients (median, 156.0 IU ml^{-1}; 25th–75th percentiles, 71.05–441.45 IU ml^{-1}, $n=137$) in the asthma cohort. These findings suggest that extrinsic allergic sensitization might have an important role in atopic asthma pathogenesis. Recent studies hypothesized skin barrier defects caused by *FLG* mutation(s) allow allergens to penetrate the skin, resulting in initiation of further immune response and leading to the development of systemic allergies, including atopic asthma (Fallon *et al.*, 2009). In patients with asthma that also harbor *FLG* mutations, we could not exclude the possibility that the systemic effects of early eczema might simply influence airway responsiveness (Henderson *et al.*, 2008).

CONFLICT OF INTEREST

Irwin McLean has filed patents relating to genetic testing and therapy development aimed at the filaggrin gene.

ACKNOWLEDGMENTS

We thank the patients and their families for their participation. We also thank Kaori Sakai for fine technical assistance and Dr James McMillan for proofreading and comments concerning this paper. This work was supported in part by Grants-in-Aid from the Ministry of Education, Science, Sports, and Culture of Japan to M Akiyama (Kiban B 20390304) and by the Health and Labour Sciences Research Grant (Research on Allergic Diseases and Immunology; H21-Meneki-Ippan-003) to H Shimizu. Filaggrin research in the McLean laboratory was supported by grants from The British Skin Foundation; The National Eczema Society; The Medical Research Council (Reference number G0700314); A*STAR, Singapore, and donations from anonymous families affected by eczema in the Tayside region of Scotland.

Rinko Osawa[1], Satoshi Konno[2], Masashi Akiyama[1], Ikue Nemoto-Hasebe[1], Toshifumi Nomura[1,3], Yukiko Nomura[1], Riichiro Abe[1], Aileen Sandilands[3], W.H. Irwin McLean[3], Nobuyuki Hizawa[4,5], Masaharu Nishimura[2] and Hiroshi Shimizu[1]

[1]Department of Dermatology, Hokkaido University School of Medicine, Sapporo, Japan; [2]First Department of Medicine, Hokkaido University School of Medicine, Sapporo, Japan; [3]Epithelial Genetics Group, Division of Molecular Medicine, University of Dundee, Colleges of Life Sciences and Medicine, Dentistry & Nursing, Dundee, UK;

[4]*Department of Pulmonary Medicine, Institute of Clinical Medicine, Graduate School of Comprehensive Human Sciences, University of Tsukuba, Tsukuba, Ibaraki, Japan and* [5]*University Hospital, University of Tsukuba, Tsukuba, Ibaraki, Japan*
E-mail: akiyama@med.hokudai.ac.jp

REFERENCES

Fallon PG, Sasaki T, Sandilands A *et al.* (2009) A homozygous frameshift mutation in the mouse *Flg* gene facilitates enhanced percutaneous allergen priming. *Nat Genet* 41: 602–8

Hanifin JM, Rajka G (1980) Diagnostic features of atopic dermatitis. *Acta Derm Venereol* 92:44–7

Henderson J, Northstone K, Lee SP *et al.* (2008) The burden of disease associated with filaggrin mutations: a population-based, longitudinal birth cohort study. *J Allergy Clin Immunol* 121:872–7

Isada A, Konno S, Hizawa N *et al.* (2010) A functional polymorphism (-603A —> G) in the tissue factor gene promoter is associated with adult-onset asthma. *J Hum Genet* 55: 167–74

Nemoto-Hasebe I, Akiyama M, Nomura T *et al.* (2010) *FLG* mutation p.Lys4021X in the C-terminal imperfect filaggrin repeat in Japanese atopic eczema patients. *Br J Dermatol* 161:1387–90

Nomura T, Akiyama M, Sandilands A *et al.* (2008) Specific filaggrin mutations cause ichthyosis vulgaris and are significantly associated with atopic dermatitis in Japan. *J Invest Dermatol* 128:1436–41

Nomura T, Sandilands A, Akiyama M *et al.* (2007) Unique mutations in the filaggrin gene in Japanese patients with ichthyosis vulgaris and atopic dermatitis. *J Allergy Clin Immunol* 119:434–40

Rodríguez E, Baurecht H, Herberich E *et al.* (2009) Meta-analysis of filaggrin polymorphisms in eczema and asthma: robust risk factors in atopic disease. *J Allergy Clin Immunol* 123:1361–70

Sandilands A, Terron-Kwiatkowski A, Hull PR *et al.* (2007) Comprehensive analysis of the gene encoding filaggrin uncovers prevalent and rare mutations in ichthyosis vulgaris and atopic eczema. *Nat Genet* 39:650–4

van den Oord RA, Sheikh A (2010) Filaggrin gene defects and risk of developing allergic sensitisation and allergic disorders: systematic review and meta-analysis. *BMJ* 339:b2433

See related commentary on pg 2703

RNase 7 Protects Healthy Skin from *Staphylococcus aureus* Colonization

Journal of Investigative Dermatology (2010) **130,** 2836–2838; doi:10.1038/jid.2010.217; published online 29 July 2010

TO THE EDITOR

The Gram-positive bacterium *Staphylococcus aureus* is an important pathogen that causes various skin infections (Miller and Kaplan, 2009). However, healthy skin is usually not infected by *S. aureus,* despite the high carrier rates in the normal population (Noble, 1998). This suggests that the cutaneous defense system has the capacity to effectively control the growth of *S. aureus.* There is increasing evidence that antimicrobial proteins are important effectors of the cutaneous defense system (Harder *et al.*, 2007). A recent study reported that keratinocytes contribute to cutaneous innate defense against *S. aureus* through the production of human β-defensin-3 (Kisich *et al.*, 2007). In addition to human β-defensin-3,, other antimicrobial proteins may also participate in cutaneous defense against *S. aureus.* One candidate is RNase 7, a potent antimicrobial ribonuclease that is highly expressed in healthy skin (Harder and Schröder, 2002; Köten *et al.*, 2009).

To investigate the hypothesis that RNase 7 may contribute to protect healthy skin from *S. aureus* colonization, we first incubated natural RNase 7 isolated from stratum corneum skin extracts (Harder and Schröder, 2002) with *S. aureus* (ATCC 6538). In concordance with our initial report about RNase 7 (Harder and Schröder, 2002), we verified that RNase 7 exhibited a high killing activity against *S. aureus* (lethal dose of 90% = 3–6 μg ml^{-1}).

Recently, we reported a moderate induction of RNase 7 mRNA expression in primary keratinocytes treated with heat-killed *S. aureus* (Harder and Schröder, 2002). To assess the induction of RNase 7 by *S. aureus* in the

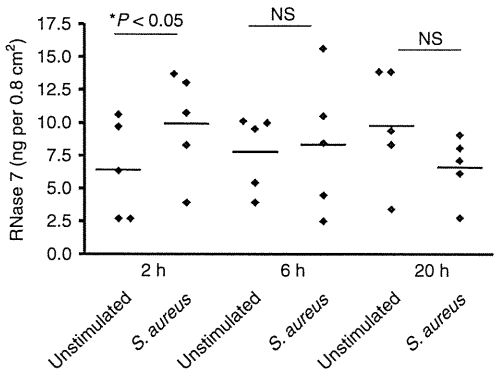

Figure 1. Induced secretion of RNase 7 on the skin surface on treatment with living *S. aureus*. Defined areas (0.8 cm^2) of skin explants derived from plastic surgery were incubated with or without approximately 1,000 colony-forming units of *S. aureus* (ATCC 6538) in 100 μl of sodium phosphate buffer. After 2, 6, and 20 hours, the concentration of secreted RNase 7 was determined by ELISA. Stimulation with *S. aureus* for 2 hours revealed a significant induction as compared with the unstimulated control after 2 hours (*P<0.05, Student's *t*-test; n.s. = not significant). Data shown are means of triplicates of five skin explants derived from five donors.

Journal of Dermatological Science 61 (2011) 38–44

Contents lists available at ScienceDirect

Journal of Dermatological Science

journal homepage: www.elsevier.com/jds

Expression of exon-8-skipped kindlin-1 does not compensate for defects of Kindler syndrome

Ken Natsuga [a,*], Wataru Nishie [a], Satoru Shinkuma [a], Hideki Nakamura [a], Yoichiro Matsushima [b], Aya Tatsuta [c], Mayumi Komine [c], Hiroshi Shimizu [a]

[a] Department of Dermatology, Hokkaido University Graduate School of Medicine, North 15 West 7, Sapporo, Japan
[b] Department of Dermatology, Sano Kosei General Hospital, Tochigi, Japan
[c] Department of Dermatology, Jichi Medical University, Tochigi, Japan

ARTICLE INFO

Article history:
Received 22 July 2010
Received in revised form 8 November 2010
Accepted 13 November 2010

Keywords:
Epidermolysis bullosa
Exon-trapping system
Basement membrane zone
Skin atrophy
Pseudo-ainhum

ABSTRACT

Background: Kindler syndrome (KS) is a rare, inherited skin disease characterized by blister formation and generalized poikiloderma. Mutations in *KIND1*, which encodes kindlin-1, are responsible for KS. c.1089del/1089+1del is a recurrent splice-site deletion mutation in KS patients.
Objective: To elucidate the effects of c.1089del/1089+1del at the mRNA and protein level.
Methods: Two KS patients with c.1089del/1089+1del were included in this study. Immunofluorescence analysis of KS skin samples using antibodies against the dermo-epidermal junction proteins was performed. Exon-trapping experiments were performed to isolate the mRNA sequences transcribed from genomic DNA harbouring c.1089del/1089+1del. β1 integrin activation in HeLa cells transfected with truncated *KIND1* cDNA was analyzed.
Results: Immunofluorescence study showed positive expression of kindlin-1 in KS skin with c.1089del/1089+1del mutation. We identified the exon-8-skipped in-frame transcript as the main product among multiple splicing variants derived from that mutation. HeLa cells transfected with *KIND1* cDNA without exon 8 showed impaired β1 integrin activation. Exon-8-coding amino acids are located in the FERM F2 domain, which is conserved among species, and the unstructured region between F2 and the pleckstrin homology domain.
Conclusion: This study suggests that exon-8-skipped truncated kindlin-1 is functionally defective and does not compensate for the defects of KS, even though kindlin-1 expression in skin is positive.

1. Introduction

Kindler syndrome (KS) is classified as a novel subtype of epidermolysis bullosa (EB) according to a revised classification of EB [1] and characterized by photosensitivity, skin fragility, fused fingers, and generalized progressive poikiloderma [2]. A characteristic histological finding in KS skin is the variability of epidermal separation and clefting at the epidermal basement membrane [3,4]. Former studies have confirmed that mutations in *COL7A1* are not a factor in KS patients [3,5].

In 2003, mutations in the *KIND1* gene encoding kindlin-1 were detected in KS patients [6,7]. The *KIND1* gene was mapped to chromosome 20p12.3 [7]. The gene spans 48.5 kb of genomic DNA and contains 14 coding sequences (exons 2–15) and one non-coding exon (exon 1) [2,7]. The *KIND1* gene is the human homolog of the *Caenorhabditis elegans* gene, *unc-112*, which encodes a membrane-associated structural/signaling protein that has been implicated in linking the actin cytoskeleton to the extracellular matrix (ECM) [7,8]. Kindlin-1 deficiency is associated with cutaneous basement membrane zone abnormalities and reduced integrin activation [9]. Also, kindlin-1 is necessary for lamellipodia formation *in vitro*, which is mediated by RhoGTPase signaling [10]. To date, more than 30 different loss-of-function mutations in *KIND1* have been reported [2].

Splicing is a common mRNA modification after transcription, in which introns are removed and exons are joined. This is mandatory for typical eukaryotic mRNA before it can be used to produce an accurate protein through translation. Nucleotide alterations in positions close to the spliced sites affect correct splicing of the mRNA transcript and result in complete skipping of the exon, retention of the intron, or the introduction of a new splice site

Abbreviations: KS, Kindler syndrome; ECM, extracellular matrix; EB, epidermolysis bullosa; SCC, squamous cell carcinoma; MASA, mutant-allele-specific amplification; PTC, premature termination codon; NMD, nonsense-mediated mRNA decay; PCR, polymerase chain reaction; DEJ, dermo-epidermal junction.

* Corresponding author. Tel.: +81 11 716 1161x5962; fax: +81 11 706 7820.
E-mail address: natsuga@med.hokudai.ac.jp (K. Natsuga).

0923-1811/$36.00
doi:10.1016/j.jdermsci.2010.11.008

within an exon or intron. Several methods are available to predict the consequences resulting from splice site mutations, such as the use of neural network software [11] (http://www.fruitfly.org/seq_tools/splice.html) and GeneSplicer software [12] (http://cbcb.umd.edu/software/GeneSplicer/). However, these programs cannot distinguish between pseudo and real splice sites [13]; therefore, other functional testing is necessary to correctly predict the mRNA products. Use of an exon-trapping system (Invitrogen, Carlsbad, CA) is one such approach for directly isolating transcribed mRNA sequences from genomic DNA [14]. This system is a reliable and easy-to-use tool for assessing the effects of splice-site mutations on mRNA splicing in cell cultures [15].

This study highlights a recurrent c.1089del/1089+1del in *KIND1* in KS patients. To elucidate the pathogenic effects of this deletion mutation on mRNA splicing, exon-trapping experiments were performed. We found that in-frame exon-8-skipped transcripts were produced by c.1089del/1089+1del defects. Immunofluorescence analysis of the patient's skin showed positive kindlin-1 staining, which might have resulted from exon-8-skipped kindlin-1. *In vitro* analysis using living cells revealed the expression of truncated kindlin-1 lead to impaired activation of β1 integrin. This study clarifies the complex sequelae resulting from a splice-site deletion mutation and provides greater understanding of the pathomechanisms involved in KS disease.

2. Materials and methods

2.1. Mutation detection

gDNA was extracted from the patient's peripheral blood cells. The mutation detection strategy was implemented after polymerase chain reaction (PCR) amplification of all exons and the intron–exon border of *KIND1*, followed by direct automated sequencing using an ABI Prism 3100 genetic analyzer (Advanced Biotechnologies, Columbia, MD). Oligonucleotide primers and PCR conditions used in this study are described elsewhere [7]. The genomic DNA nucleotides, the complementary DNA nucleotides, and the amino acids of the protein were numbered based on the following sequence information: GenBank accession no. NM_017671 [7].

2.2. Mutant-allele-specific amplification analysis

To verify the c.1761T>A mutation, using PCR products as a template, mutant-allele-specific amplification (MASA) analysis was performed with mutant-allele-specific primers carrying the substitution of two bases at the 3′-end mutant-allele-specific primers [16,17]: forward, 5′-ACATTCTGGGAGTTTCATGA-3′; reverse, 5′-CAATTCTGAGGGACACACAT-3′. Only the 179-bp fragment derived from the mutant allele was amplified with these primers.

2.3. Electron microscopy

Electron microscopy was performed as previously described [18,19]. Briefly, skin biopsy samples were fixed in 2% glutaraldehyde solution, post-fixed in 1% OsO_4, dehydrated, and embedded in Epon 812. The samples were sectioned at 1 μm thickness for light microscopy and thin sectioned for electron microscopy (70 nm thick). The thin sections were stained with uranyl acetate and lead citrate, and examined in a transmission electron microscope.

2.4. Antibodies

The following antibodies (Abs) were used: monoclonal antibody (mAb) HD1-121 against the rod domain of plectin; mAbs GoH3 and 3E1 against α6 and β4 integrins, respectively (Chemicon International, CA); mAb GB3 against laminin 332 (Sera-lab, Cambridge, UK); mAb LH7.2 against type VII collagen (Sigma, St. Louis, MO); mAb PHM-12+CIV22 against type IV collagen (NeoMarkers, Fremont, CA); S1193 against BP230; mAb HDD20 against type XVII collagen; anti-kindlin-1 Ab (ab68041) that recognizes the C-terminus of kindlin-1 (Abcam, Cambridge, UK); unconjugated and horseradish peroxidase conjugated anti-V5 Abs (Invitrogen); and mAbs 4B7R and 12G10 against β1 integrin (Abcam, Cambridge, UK). The following secondary antibodies were used: fluorescein isothiocyanate (FITC)-conjugated goat anti-rabbit Ab (Jackson Immuno Research, West Grove, PA); FITC-conjugated goat anti-mouse Ab (Jackson Immuno Research); and TIRTC-conjugated goat anti-mouse Ab (SouthernBiotech, Birmingham, AL); horseradish peroxidase-conjugated goat anti-mouse Ab (Jackson Immuno Research). mAb GoH3 was a kind gift from Dr. A. Sonnenberg of the Netherlands Cancer Institute. mAbs HD1-121 and HDD20 were kind gifts from Dr. K. Owaribe of Nagoya University. The antibody S1193 was a kind gift from Dr. J.R. Stanley of the University of Pennsylvania.

2.5. Skin immunofluorescence studies

Indirect immunofluorescence analysis using a series of antibodies against antigens at the dermo-epidermal junction (DEJ) and cryostat skin sections was performed as previously described [3,20].

2.6. Exon-trapping experiments

Exon-trapping (Invitrogen, Carlsband, CA) is an approach used for the direct isolation of mRNA sequences transcribed from gDNA. To generate a *KIND1* genomic fragment extending from intron 6 to intron 9, we synthesized two primers (5′-GAATTCCTGAGCTGAAGTTTGCTGCA-3′ and 5′-GGATCCACCTTTGAACCATGAACCTG-3′) which contained the respective restriction enzyme sites: EcoRI and BamHI. PCR were performed using the patient's gDNA as a template. The DNA fragment was digested with EcoRI and BamHI and subcloned into the multi-cloning site of a pSPL3 expression vector, which contained a portion of the HIV-1 tat gene, an intron, splice donor and acceptor sites, and some flanking exon sequences. Sequence analysis selected constructs with or without the splice site mutation c.1089del/c.1089+1del. The constructs were transfected into HaCaT cells using lipofectamine LTX (Invitrogen) according to the manufacturer's instructions. Total RNA was extracted from the cultured cells and RT-PCR was performed using the trapping vector-specific oligonucleotide primers. The samples without transfection of the SPL3 were used as controls. The PCR products were subcloned into a TA cloning vector pCRII (Invitrogen).

2.7. In vitro analysis of truncated KIND1

cDNA containing the entire coding region of *KIND1* (FEMT1wt) was subcloned into the pcDNA3.1V5-His vector (Invitrogen). *KIND1* cDNA without exon 8 was subcloned to generate the same vector minus exon 8 (KIND1delex8) using PCR methods and the following flanking *KIND1* cDNA primers: sense, 5′-GAGGACATTACTGATATCCC-3′, anti-sense, 5′-CTGTAGAGCTGCAAAGATCA-3′. Two different KIND1wt and KIND1delex8 transfections were performed into HeLa cells, using Lipofectamine LTX (Invitrogen). For immunoblotting, HeLa cells 24 h after transfection were lysed in Laemmli buffer [21], cell debris was removed by centrifugation, and supernatant was collected. SDS-PAGE and immunoblotting were performed using standard techniques. For immunofluorescence, HeLa cells at 24 h after transfection were washed with phosphate-buffered saline and fixed with methanol. All cells were observed using a confocal laser scanning microscope (Olympus Fluoview FV300).